공학석사 학위논문

Prediction and Modelling of Extreme Sloshing Pressures on Liquid Cargo

액체 화물창 내 슬로싱 극한 충격압력의 예측 및 모델링

2017년 8월

서울대학교 대학원

조선해양공학과

Ekin Ceyda Cetin

Abstract

Prediction and Modelling of Extreme Sloshing Pressures on Liquid Cargo

Ekin Ceyda Cetin
Department of Naval Architecture and Ocean Engineering
The Graduate School
Seoul National University

Sloshing is a well-known phenomenon that has attracted attention of researches over the last few decades. Sloshing in LNG cargo tanks had a new turn with changes in the LNG market at the end of 1990's. As a result, increase in tanks sizes and changes in operational conditions were inevitable which brought some technical concerns regarding sloshing problem. There are a great number of studies in the area of sloshing including analytic, experimental and numerical studies. Since sloshing is a complex liquid motion, the computational effect required for numerical analysis is very high. Therefore, experimental method is widely used in determination of slosh-induced loads.

Accurate prediction of maximum pressure in a designated return period is a crucial step in structural design of LNG cargo containment system. In order to determine the maximum pressure, statistical post-processing must be carried out. In this step, it is important that an appropriate statistical distribution is used to describe the peak pressures. Traditionally, Weibull and generalized Pareto models are used in short term prediction; however, there is

a need for a wider investigation in this area to find better alternatives for long term prediction.

Another issue about sloshing impact pressures is the idealization of peak pressure signals. In the current procedure, peak pressure signals are modelled as triangular shapes for the simplicity of structural analysis. Triangular modelling that passes through rise and decay times at a certain ratio of peak pressure value is used most commonly. Since accurate modelling of peak pressure signals and determination of rise and decay time are significant in terms of structural response, the modelling of peak pressure signals must be studied in more detail.

In this thesis, statistical analysis of sloshing impact pressures is carried out. To this end, various statistical models are applied to peak pressure data which were acquired from sloshing models tests of 5hrs duration (in real scale) repeated 20 times in 3 filling levels, and, for further analysis, the best 4 distributions are chosen which are Weibull, generalized Pareto, generalized extreme value and log-logistic distributions. Using different distribution fitting methods, these statistical models are applied to the data sets of peak pressures. The fits are evaluated using probability-of-exceedance curves and goodness-of-fit tests according to different filling levels. Another evaluation is carried out by comparing the squared error between accumulated peak pressure data (100hrs test data) and short duration test data (5hrs test data) fittings in different zones of return period. This evaluation results are also displayed in long term, being plotted to understand the behaviors of distributions in case of long term prediction. In addition, taking 100hrs test data as a reference, another comparison is made for the current short term prediction procedure of the classification societies.

In the next part of the thesis, analysis on triangular modelling of impact pressure signals is carried out. The rise and decay times in 9 stations of

pressure signals are extracted and utilized for comparing different pressure ratios of triangular signal modelling. The summed absolute difference between the rise and decay times in actual signal and modelled signal are calculated in these 9 stations. The comparison of pressure ratios are displayed in different percentages of highest peak pressures in each filling level. Considering the results, a suggestion is made for pressure ratio of triangular signal modelling.

Keywords: Sloshing, impact pressures, statistical analysis, sloshing experiment, signal modelling.

Student Number: 2015-23297

Contents

List of Tables

List of Figures

1. Introduction

Sloshing is a well-known phenomenon that occurs in partially filled LNG tanks. Sloshing in LNG cargo tanks had a new turn with changes in the LNG market at the end of 1990's. Due to the growing demand of LNG in the world, the demand for larger LNG carriers also increased. While modest LNG carriers up to 145,000 m^3 capacity were built in the 1970's to 1990's, the capacity of ships built after 2000 are up to 280,000 m^3. With larger ships and mostly the same number of tanks, the increase in the tank size was inevitable for efficient and economic operation. Moreover, LNG market being a spot market brought concerns about filling restrictions. In order to have the flexibility of partially loaded operation, sloshing in intermediate filling levels also started to draw attention of researchers. With the spreading of the floating production storage and offloading platforms (FPSOs), LNG carriers face more harsh weather conditions during loading and offloading operations. All in all, these changes in the LNG market effects the design of the cargo containment systems in LNG carriers, raising some technical issues in sloshing in LNG tanks.

Sloshing has attracted attention of researches over the last few decades. There are numbers of numerical studies regarding estimation of sloshing pressures in membranes. Since sloshing is a highly stochastic and complex motion which includes phenomenon such as splash and wave breaking, it requires a great computational effort to calculate the sloshing impact pressures which occurs in small areas of the tank. Therefore, experimental method is widely used in determination of slosh-induced loads as well as in validation of numerical simulations. Once sloshing experiment is conducted and pressure signals are received, statistical post-processing must be carried out in order to acquire design sloshing load from peak pressures. Mathiesen (1976) and Gran (1981) are the two fundamental researches in this

area, applying a statistical approach to estimate the design sloshing loads. Mathiesen applied Weibull distribution to peak pressure data acquired from random pitch motion while Gran applied Weibull and Frechet distributions to peak pressures and compared both results. In Graczyk et al. (2006), statistical analysis of 5hrs sloshing model tests are carried out, applying Weibull and Generalized Pareto models to the sets of peak pressure data. In the study, a procedure for sloshing experiments is presented as well as discussions about spatial and temporal characteristics of pressures and model scaling problem. Kuo et al. (2009) gathers basic challenging issues in LNG sloshing including statistical modelling of maximum sloshing pressures and estimation of confidence bounds. Fillon et al. (2011) focuses on statistical post-processing of experimental data by fitting generalized extreme value, three-parameter Weibull and generalized Pareto distributions to peak pressures and using Kolmogorov-Smirnov goodness-of-fit test and confidence intervals to evaluate these fittings.

Accurate prediction of maximum pressure in a designated return period is a crucial step in structural design of LNG tanks. Estimated maximum pressure changes significantly according to which statistical distribution is used in mathematical description of peak pressures. In the current application, Weibull distribution and generalized Pareto distribution are mostly used to estimate the maximum pressure. In short term prediction, different distributions may return closer estimates. However, recently long term prediction has attracted interest as it considers the weather conditions that the ship may endure during its life-time. In long term prediction, distribution selection and even choice of distribution fitting method can create a great difference. Therefore, there is a need for wider investigation on other statistical models to find better alternatives for estimating the pressure value in longer return periods.

Another issue about sloshing impact pressures is the idealization of peak pressure signals. In the current procedure, peak pressure signals are modelled as triangular shapes in pressure time histories for the simplicity of structural analysis. There are a smaller number of studies regarding the modelling of sloshing peak pressure signals. Kim et al. (2014) classified the current modelling methods used by classification societies and research facilities as Type 1 and Type 2. Type 1 is the triangular modelling passing through rise and decay time values at the pressure threshold and Type 2 is the triangular modelling passing through rise and decay times at a certain ratio of peak pressure value. Kim et al. investigated rise and decay times in each modelling type as well as their effect on impulse area modelling. Graczyk and Moan (2008) investigated the accuracy of triangular modelling and proposed a trapezoidal modelling as an alternative approach.

Modelling of peak pressure signals is significant in terms of structural response. The structural response is dependent on the magnitude of pressure as well as the duration of the impulse. The highest peak pressure does not necessarily cause the highest structural response, but a longer duration impact with small magnitude of pressure may. The rise and decay times are used in the impulse area modelling, which also effects structural response. The selection of rise time should also consider the natural resonances of tanks and the ship, and rise times near these resonances may need to be investigated (Lloyd's Register, 2009). Therefore, accurate idealization of pressure signals is of high importance in analysis of sloshing impact pressures and should be further investigated.

In this thesis, statistical analysis of sloshing impact pressures is carried out. The peak pressures data acquired from sloshing models tests of 5hrs duration (in real scale) repeated 20 times in 3 filling levels is used. Various statistical models are applied to peak pressure data and, for further

analysis, the best 4 distributions are chosen which are Weibull, generalized Pareto, generalized extreme value and log-logistic distributions. Using different distribution fitting methods, these statistical models are applied to data sets of peak pressure. The fits are evaluated using probability-of-exceedance curves and goodness-of-fit tests (probability plot correlation coefficient test) according to different filling levels. Another evaluation is carried out by comparing squared error between accumulated peak pressure data (100hrs test data) and short duration test data (5hrs test data) fittings in different zones of return period. This evaluation results are also displayed in long term plotting to understand the behavior of distributions in case of long term prediction. In addition, taking 100hrs test data as a reference, another comparison is made according to the current short term prediction procedure of the classification societies.

In the next part of the thesis, analysis on triangular modelling of impact pressures is carried out. The rise and decay times in 9 stations of pressure signals are extracted and utilized in comparison of different pressure ratios of Type 2 triangular signal modelling. The summed absolute difference between the rise and decay times in actual signal and modelled signal are calculated in these 9 stations. The comparison of pressure ratios are displayed in different percentages of highest peak pressures in each filling level. Considering the results, a suggestion is made for pressure ratio of triangular signal modelling.

2. Mathematical Model & Approaches

2.1. Statistical Analysis of Peak Pressures

2.1.1. Statistical Distributions

The peak pressures acquired from 20 repetitions of 5hrs (in real scale) sloshing model test are used in this thesis and each 5hrs test is referred to as one case. Peak pressures are extracted from pressure signals according to the time window, 0.2 ms and pressure threshold, 2.5 kPa (Kim, 2017).

In order to estimate the maximum pressure, statistical distributions are applied to the peak pressure data and pressure value corresponding to chosen return period is determined as the maximum pressure. The current procedure according to classification societies is that applying Weibull or generalized Pareto distributions to the peak pressure data and to choose the pressure value corresponding to 3-hour return period as the maximum pressure. The distributions used by different classification societies are shown in Table 2.1.

Table 2.1 Statistical models currently used by classification societies

Organization	**Statistical Distribution**
BV	Generalized Pareto distribution
	Weibull distribution
	Generalized extreme value distribution
ABS	Weibull distribution
DNV	Weibull distribution
	Generalized Pareto distribution
LR	Weibull distribution
	Generalized Pareto distribution
	Log-normal Distribution

11 statistical distributions are used in the first step of the research as shown in Table 2.2. An evaluation based on probability of exceedance curves and chosen goodness-of-fit tests is carried out and the best 4 distributions are determined for further study, which are Weibull distribution, generalized Pareto distribution, generalized extreme value distribution, log-logistic distribution.

Table 2.2 Statistical distributions applied in the first step

Statistical Distributions for the First Step
Weibull distribution
Generalized Pareto distribution
Generalized extreme value distribution
Log-logistic distribution
Logistic distribution
Log-normal distribution
Birnbaum-Saunders distribution
Gamma distribution
Inverse-Gaussian distribution
Nakagami distribution
Rician distribution

Weibull distribution (WBL) is widely used in the statistical analysis of sloshing impact pressures. The probability density function, *f(x)* and the cumulative distribution function, *F(x)* are given as follows.

$$f(x \mid \gamma, \theta, \beta) = \frac{\gamma}{\beta}\left(\frac{x-\theta}{\beta}\right)^{\gamma-1} \exp\left(-\left(\frac{x-\theta}{\beta}\right)^{\gamma}\right) \tag{1}$$

$$F(x \mid \gamma, \theta, \beta) = 1 - \exp\left(-\left(\frac{x-\theta}{\beta} \right)^{\gamma} \right) \tag{2}$$

In these functions, γ is the shape parameter, θ is the location parameter, β is the scale parameter and variable *x* should be equal or larger than the shape parameter.

Generalized Pareto distribution (GP) is also widely used in estimation of maximum pressure value in sloshing. The probability density function, *f(x)* and the cumulative distribution function, *F(x)* are given as follows.

$$f(x \mid \gamma, \beta) = \left(\frac{1}{\beta} \right) \left(1 + \frac{\gamma x}{\beta} \right)^{-1-\frac{1}{\gamma}} \tag{3}$$

$$F(x \mid \gamma, \beta) = 1 - \left(1 + \frac{\gamma x}{\beta} \right)^{-\frac{1}{\gamma}} \tag{4}$$

In these functions, γ is the shape parameter and β is the scale parameter. Generalized Pareto distribution usually applied to tail of the data to acquire a better fit. Therefore, Peak-Over-Threshold Method is adapted which only the data that exceeds a certain threshold value is taken into consideration. Considering a sample of x_i, $i=1,.,n$ with sample size *n* and *G(x)* is the distribution function and we are interested in *k* $(k<n)$ peaks which exceed a threshold *u*. This sample of size *k* is called peaks over threshold and denoted X_i, $i=1,.,k$ $(X_i>u)$. The distribution of the X_i is given as,

$$G_X(x) = P\left[X \le x \mid X > u \right] = \begin{cases} 0 & \text{if} \quad x \le u \\ \dfrac{G(x) - G(u)}{1 - G(u)} & \text{if} \quad x > u \end{cases} \tag{5}$$

And the distribution function of the excesses, i.e. the amounts by which the peaks exceed threshold, is given as

$$G_{X-u}(x) = P\left[(X-u) \le x \mid X > u\right] = P\left[X \le (x+u) \mid X > u\right]$$
$$= \frac{G(x+u) - G(u)}{1 - G(u)} \tag{6}$$

$F_{X\text{-}u}(x)$ is the probability that a peak exceeds the threshold u by no more than an amount x, given that the threshold is exceeded. The relation between the two distribution functions is

$$G_{X-u}(x) = G_X(x+u) \tag{7}$$

Pickand's theorem implies that the distribution function of the excesses $G_{X\text{-}u}(x)$ may be modelled by $F(x|\gamma,\beta)$ and the distribution function of peaks over u,

$$G_X(u) = F_{X-u}(x-u) = F(x-u \mid \gamma, \beta) \tag{8}$$

provided that u is sufficiently high (Pickands, 1975).

The initial peak distribution in the tail part $G(x)$ when $x>u$ may be obtained by rewriting $G(x)$ as

$$G(x) = G_X(x)\left[1 - f(u)\right] + F(u) \qquad (x > u). \tag{9}$$

$G_X(x)$ can be modelled by the generalized Pareto distribution function $F(x|\gamma,\beta)$ and $G(u)$ can be approximated by the empirical probability, which is the number of data points less than or equal to u divided by the number of samples n

$$\hat{G}(u) = \frac{1}{n}\sum_{i=1}^{n} 1_{X_i \le u} \tag{10}$$

This gives

$$G(x) = F(x-u \mid \gamma, \beta)\left[1 - \hat{G}(u)\right] + \hat{G}(u) \qquad (x > u). \tag{11}$$

This implies that the initial peak distribution in the tail part can be calculated from the fitted generalized Pareto distribution and empirical probability $\hat{G}(u)$ (Rognebakke et al., 2005).

Although, generalized Pareto distribution is fitted to the tail data, the parameters for the whole data can be obtained. The shape parameter γ does not change. The scale parameter $\hat{\beta}$ and location parameter $\hat{\theta}$ is calculated as

$$\hat{\beta} = \beta\left(1-\hat{G}(u)\right)^{\gamma} \tag{12}$$

$$\hat{\theta} = u - \frac{\hat{\beta}\left(\left(1-\hat{G}(u)\right)^{-\gamma} - 1\right)}{\gamma} \tag{13}$$

In this thesis, the 0.92 quantile of the sample peaks is considered as the threshold value which means 8% largest peaks are considered.

The probability density function, *f(x)* and the cumulative distribution function, *F(x)* of generalized extreme value distribution (GEV) are given as follows.

$$f(x\,|\,\gamma,\theta,\beta) = \left(\frac{1}{\beta}\right)\exp\left(-\left(1+\gamma\frac{(x-\theta)}{\beta}\right)^{-\frac{1}{\gamma}}\left(1+\gamma\frac{(x-\theta)}{\beta}\right)^{-1-\frac{1}{y}}\right) \tag{14}$$

$$F(x\,|\,\gamma,\theta,\beta) = \exp\left(-\left(1+\gamma\frac{(x-\theta)}{\beta}\right)^{-\frac{1}{\gamma}}\right) \tag{15}$$

In these functions, γ is the shape parameter, θ is the location parameter, β is the scale parameter and variable *x* should be equal or larger than the shape parameter. If shape parameter of generalized extreme value distribution is negative, Weibull distribution is a reverse generalized extreme value distribution.

The three parameter log-logistic (LL) distribution, also known as generalized logistic distribution, is often used in estimating flood frequencies in hydrology. There is no application of log-logistic distribution in sloshing peak pressures, yet. The probability density function, *f(x)* and the cumulative distribution function, *F(x)* are given as follows.

$$f(x\,|\,\gamma,\theta,\beta)=\frac{\left(1-\gamma\left(\frac{x-\theta}{\beta}\right)\right)^{\frac{1}{\gamma}-1}}{\beta\left[1+\left(1-\gamma\left(\frac{x-\theta}{\beta}\right)\right)^{\frac{1}{\gamma}}\right]^{2}} \tag{16}$$

$$F(x\,|\,\gamma,\theta,\beta)=\left[1+\left(1-\gamma\left(\frac{x-\theta}{\beta}\right)\right)^{\frac{1}{\gamma}}\right]^{-1} \tag{17}$$

There is also an alternate parameterization as given below, which is preferable in some cases due to more interpretable values of parameters.

$$f(x\,|\,\gamma,\theta,\beta)=\frac{\gamma\left(\frac{x-\theta}{\beta}\right)^{\gamma-1}}{\beta\left(1+\left(\frac{x-\theta}{\beta}\right)^{\gamma}\right)^{2}} \tag{18}$$

$$F(x\,|\,\gamma,\theta,\beta)=\left(1+\left(\frac{\beta}{x-\theta}\right)^{\gamma}\right)^{-1} \tag{19}$$

In these functions, γ is the shape parameter, θ is the location parameter, β is the scale parameter and variable *x* should be equal or larger than the shape parameter. In this thesis, alternate parameterization is used for method-of-moments and maximum-likelihood-estimation while normal parameterization

is used for l-moments method. Even if the parameter values are different, both functions return the same fits with the same parameter estimation method.

The probability of exceedance function is calculated as, *1-F(x)* where *F(x)* is the cumulative distribution function. The probability of exceedance curves are plotted in log-scale in y-axis for a better observation of extreme values in tail. In the x-axes of probability of exceedance curves, normalized pressure values are plotted. Normalized pressure value is calculated as $P/\rho gH$ where P is the magnitude of pressure, ρ is the density, g is the gravity and H is the height of the tank. In order to obtain the maximum pressure value corresponding to a certain return period, $Q(N)$ is used where Q is the inverse-cumulative distribution function (quantile function) and N is the number of samples measured in m hours. If n is the number of samples measured in t seconds, N is calculated as below.

$$N = \frac{3600nm}{t} \tag{20}$$

2.1.2. Distribution Fitting Methods

In the distribution fitting process, it is seen that different estimation methods can lead to very different parameter estimates for some distributions and slightly different estimates for some. This affects the estimated maximum pressure value either significantly or slightly. Fitting methods are directly related to goodness-of-fit and can be considered as a parameter that changes the fitted distribution. Thus, this study adopts multiple parameter estimation methods as to examine a wider range of fits. Therefore, 3 different distribution fitting methods are applied in order to estimate the distribution parameters, which are maximum likelihood estimation (MLE), method-of-moments (MOM) and l-moments method (LMOM). However, some methods may not

be suitable for certain distributions. These limitations and the reasons are explained for each distribution fitting method in this part.

Maximum likelihood estimation, originally developed by R. A. Fisher in the 1920's, is a method to find the probability distribution that makes the observed data most probable by maximizing the likelihood function. Likelihood function is defined as,

$$L(w \mid x) = f(x \mid w) \tag{21}$$

where L is the likelihood function, f is the probability density function of the distribution and w is the distribution parameter. Instead of likelihood function, negative log-likelihood function is used for computational convenience. For each statistical model, negative log-likelihood function is calculated from probability density function and an optimization to minimize this function is executed. It should be noted that, MLE can return biased estimates for small sample sizes. For WBL, MLE is applicable only when shape parameter is greater than one (Smith, 1985). However, in the case of peak pressures, shape parameter is usually smaller than one. Therefore, MLE is not suitable to use in this study. A weighted-maximum likelihood estimation method proposed by Cousineau (2009), was used for WBL parameter estimation which inserts 3 weights in the log-likelihood function. This method requires 2^{20} Monte-Carlo simulations to estimate the weights in order to obtain a decent fit. Since it requires too much time, especially for large sample sizes over 1000, this method is inconvenient for the case of peak pressures.

Method-of-moments (MOM) uses summary statistics to estimate the parameters by matching the first three model moments –mean, variance and skewness- with their corresponding sample moments. The mean ($\hat{\mu}$), variance ($\hat{\sigma}^2$) and skewness ($\hat{\gamma}_1$) of the sample data are given as follows.

$$\hat{\mu} = \frac{1}{n}\sum_{i=1}^{n} x_i \tag{22}$$

$$\hat{\sigma}^2 = \frac{1}{n-1}\sum_{i=1}^{n} (x_i - \hat{\mu})^2 \tag{23}$$

$$\hat{\gamma}_1 = \frac{1}{n}\sum_{i=1}^{n} \left(\frac{x_i - \hat{\mu}}{\hat{\sigma}} \right)^3 \tag{24}$$

The mean (μ), variance (σ^2) and skewness (γ_1) of Weibull distribution:

$$\mu = \beta\, \Gamma\left(1 + \frac{1}{\gamma}\right) + \theta \tag{25}$$

$$\sigma^2 = \beta^2 \left[\Gamma\left(1 + \frac{2}{\gamma}\right) - \Gamma^2\left(1 + \frac{1}{\gamma}\right) \right] \tag{26}$$

$$\gamma_1 = \frac{\Gamma\left(1 + \frac{3}{\gamma}\right) - 3\Gamma\left(1 + \frac{1}{\gamma}\right)\Gamma\left(1 + \frac{2}{\gamma}\right) + 2\Gamma^3\left(1 + \frac{1}{\gamma}\right)}{\left[\Gamma\left(1 + \frac{2}{\gamma}\right) - \Gamma^2\left(1 + \frac{1}{\gamma}\right) \right]^{3/2}} \tag{27}$$

The mean (μ) and variance (σ^2) of generalized Pareto distribution:

$$\mu = \frac{\beta}{1-\gamma} \tag{28}$$

$$\sigma^2 = \frac{\beta^2}{(1-2\gamma)(1-\gamma)^2} \tag{29}$$

The mean (μ), variance (σ^2) and skewness (γ_1) of log-logistic distribution which used with alternate parameterization:

$$\mu = \beta \frac{\pi}{\gamma} \csc\left(\frac{\pi}{\gamma}\right) + \theta \tag{30}$$

$$\sigma^2 = \beta^2 \frac{\pi}{\gamma}\left[2\csc\left(\frac{2\pi}{\gamma}\right) - \frac{\pi}{\gamma}\csc^2\left(\frac{\pi}{\gamma}\right)\right] \tag{31}$$

$$\gamma_1 = \frac{3\csc\left(\frac{3\pi}{\gamma}\right) - 6\frac{\pi}{\gamma}\csc\left(\frac{2\pi}{\gamma}\right)\csc\left(\frac{\pi}{\gamma}\right) + 2\left(\frac{\pi}{\gamma}\right)^2 \csc^3\left(\frac{\pi}{\gamma}\right)}{\sqrt{\frac{\pi}{\gamma}\left[2\csc\left(\frac{2\pi}{\gamma}\right) - \frac{\pi}{\gamma}\csc^2\left(\frac{\pi}{\gamma}\right)\right]^{3/2}}} \tag{32}$$

where x_i stands for i-th peak value when the peaks are ordered in ascending order, n for sample size and Γ for the Gamma function. MOM can be limiting when second of higher moments are only define for a certain range of shape parameter. In case of GEV, the mean and variance of GEV are infinite for the cases which shape parameter is greater than 1 and 1/2, respectively. Since parameter estimation is not possible for shape parameters in these specified ranges, MOM method is not applied for GEV in this study.

L-moments method (LMOM), described by Hosking (1990), uses L-moments to obtain the distribution parameter and is an alternative approach to method-of-moments. L-moments are analogous to the conventional moments but can be estimated by linear combinations of order statistics. Similar to MOM, LMOM matches L-moments and L-moments ratios of the distribution with their corresponding sample L-moments and L-moment ratios. The sample l-moments l-location (l_1), l-scale (l_2) and sample l-moments ratios l-skewness (t_3) and l-kurtosis (t_4) are calculated using probability weighted moments and the coefficients of the shifted Legendre polynomial showed by Hosking et al. (1985).

$$l_r = \sum_{k=0}^{r-1} p^*_{r-1,k} b_k \tag{33}$$

$$b_k = n^{-1}\sum_{i=1}^{n}\frac{(i-1)(i-2)...(i-r)}{(n-1)(n-2)...(n-k)}x_{i:n} \tag{34}$$

$$p^*_{r,k} = (-1)^{r-k}\binom{r}{k}\binom{r+1}{k} \tag{35}$$

$$t_r = \frac{l_r}{l_2} \tag{36}$$

where $X_{1:n} \leq X_{2:n} \leq \cdots \leq X_{n:n}$ indicates ordered sample, $p*$ is the coefficients of the shifted Legendre polynomial.

The l-location (λ_1), l-scale (λ_2) and l-skewness (τ_3) of Weibull distribution:

$$\lambda_1 = \theta + \beta\,\Gamma\left(1+\frac{1}{\gamma}\right) \tag{37}$$

$$\lambda_2 = \beta\left(1-2^{-1/\gamma}\right)\Gamma\left(1+\frac{1}{\gamma}\right) \tag{38}$$

$$\tau_3 = 3-\frac{2\left(1-3^{-1/\gamma}\right)}{1-2^{-1/\gamma}} \tag{39}$$

The l-location (λ_1), l-scale (λ_2) and l-skewness (τ_3) of generalized extreme value distribution:

$$\lambda_1 = \theta + \frac{\beta}{\gamma}\left(1-\Gamma\left(1+\gamma\right)\right) \tag{40}$$

$$\lambda_2 = \frac{\beta}{\gamma}\Gamma\left(1+\gamma\right)\left(1-2^{-\gamma}\right) \tag{41}$$

$$\tau_3 = 2\frac{\left(1-3^{-\gamma}\right)}{\left(1-2^{-\gamma}\right)}-3 \tag{42}$$

The l-location (λ_1), l-scale (λ_2) and l-kurtosis (τ_4) of log-logistic distribution used with normal parameterization:

$$\lambda_1 = \theta + \frac{\beta}{\gamma}\left(1 - \Gamma\left(1+\gamma\right)\Gamma\left(1-\gamma\right)\right) \tag{43}$$

$$\lambda_2 = \beta\ \Gamma\left(1+\gamma\right)\Gamma\left(1-\gamma\right) \tag{44}$$

$$\tau_4 = \frac{1+5\gamma^2}{6} \tag{45}$$

Estimation methods used for each distribution and the notation for each fit are shown in Table 2.3.

Table 2.3 Parameter estimation methods applied to each distribution.

Distribution	**Method**	**Notation**
Weibull distribution	Method-of-moments	WBL-MOM
	L-moments method	WBL-LMOM
Generalized Pareto distribution	Method-of-moments	GP-MOM
	Maximum-likelihood estimation	GP-MLE
Generalized extreme value distribution	L-moments method	GEV-LMOM
	Maximum-likelihood estimation	GEV-MLE
Log-logistic distribution	Method-of-moments	LL-MOM
	Maximum-likelihood estimation	LL-MLE
	L-moments method	LL-LMOM

2.1.3. Goodness-of-Fit Test

To examine the goodness-of-fit, probability plot correlation coefficient test (PPCC test) is used. PPCC test was first proposed by Filiben (1975) for normal distribution and it was developed to be applied in other distributions in studies after that. This test uses the correlation coefficient r between the ordered observations X_i and fitted quantiles M_i determined by plotting positions p_i for each X_i. It is assumed that the observations could have been drawn from the fitted distribution if the value of r is close to 1.0. Essentially, r measures the linearity of the probability plot, providing a quantitative assessment of fit (Heo at al., 2008). The correlation coefficient r is defined as,

$$r = \frac{\sum_{i=1}^{n}\left(X_i - \bar{X}\right)\left(M_i - \bar{M}\right)}{\sqrt{\sum_{i=1}^{n}\left(X_i - \bar{X}\right)^2 \sum_{i=1}^{n}\left(M_i - \bar{M}\right)^2}} \tag{46}$$

where $\bar{X}$ and $\bar{M}$ denote the mean values of the observations X_i and the fitted quantiles M_i, respectively and n is the sample size. The estimate of order statistic median for M_i is shown as

$$M_i = \Phi^{-1}(m_i) \tag{47}$$

$$m_i = 1 - (0.5)^{1/n}, \qquad i = 1$$

$$m_i = \frac{i - 0.44}{n + 0.12}, \qquad i = 2, \ldots, n-1 \tag{48}$$

$$m_i = (0.5)^{1/n}, \qquad i = n$$

where Φ^{-1} is the inverse of cumulative distribution function and m_i are the median values. Plotting position formula used in this study is suggested by Cunnane (1978) for WBL and LL. There are other plotting positions suggested for GP and GEV each in different studies. However, it was observed in the goodness-of-fit test results that using different plotting positions for different distributions does not provide a healthy comparison of PPCC values. Therefore, the same plotting positions are adapted for all fits. Judging by the way it is calculated, PPCC test is sensitive to sample size in different parts of the distribution.

For hypothesis testing, critical values are calculated from Monte-Carlo simulations. 10^5 random samples, which have the same sample size of the peak pressure data, are generated from fitted distributions and PPCC is calculated for each one of these random samples. Significance level is chosen as 0.05. Therefore $(10^5 \times (1-0.05))^{th}$ highest PPCC value is chosen as the critical value (Vogel, 1986). If the PPCC of the pressure data is higher than the critical value, then hypothesis return 0 which means that, in that certain significant level, the data is drawn from the distribution and otherwise returns 1.

Since the data from 5hrs test (in real scale) repeated 20 times for each filling level is used in this thesis, a ranking method is needed to organize the results of PPCC test of each case, according to panels and filling levels. That is, for each case (5hrs test), distributions are ranked from 1 to 9 according to the value of PPCC where 9 is appointed to the best fit, 1 to the worst fit and the fits in between accordingly. In each panel, mean ranking of each fit is calculated for 20 tests. In each filling level, mean ranking is calculated for 4 panels. The results are displayed in % to show the share of each fit, 100% being total rank of all the fits. The results are displayed separately for

different filling levels, because each filling level is thought to have their own pattern of the peak pressures distribution.

As useful as goodness-of-fit tests are, observation of the POE curves are also an adequate method to see how the statistical model behaves, even though it lacks of numerical display.

2.1.4. Squared Error

Goodness-of-fit test are useful to evaluate how well the fit follows the sample data. However, if long term prediction is the interest, how well short duration test fittings follow the long duration test data gains importance. The reason for that is, in the actual procedure, usually 5hrs test is repeated one or two times and the data acquired from these tests are used in estimation of maximum pressure. Most of the time, long duration test is not an option. Since sloshing is a highly stochastic phenomenon, the peak pressure data acquired from sloshing model tests remains random. However, accumulated data from repeated tests, long duration test data, is more converged than short duration test data. Thus, fewer outliers are seen in the long duration test data comparing to short duration test data. In addition, for the pressure values corresponding to shorter return periods, the data are converged enough that the outliers in short duration test data are mostly eliminated. Taking test data directly as a reference can be discussed in different points of view. The most obvious argument is that distribution fitting is carried out so that test data itself is not used for estimation of maximum pressure. The test data remains random; this is why we try to acquire a mathematical description of peak pressures. This is a valid argument. For this reason, the idea is not to use long duration test data for direct estimation of maximum pressure. Instead, the test data will provide a converged guidance for return periods that are shorter than

the duration of the test as well as providing an idea for long term prediction. Therefore, 100hrs experiment data is taken as a reference in this part to compare the behavior of different 5hrs data fits in the long term prediction.

In order to have a detailed comparison, 100hrs experiment data is divided into zones of return periods (Table 2.4).

Table 2.4 Zones of return periods (real scale)

Zone	**Return Period**
Zone 1	~ 3-hour
Zone 2	3-hour – 5-hour
Zone 3	5-hour – 10-hour
Zone 4	10-hour – 100-hour

Squared error (ε_i) between the fitted distributions and 100hrs experiment data is calculated as

$$\varepsilon_i = \frac{\sum_{1}^{n_i} \left| P_{\text{reference}} - P_{\text{estimated}} \right|^2}{n_i} \qquad i = 1, 2, 3, 4 \ (zones) \tag{49}$$

where n_i is the sample size in Zone i and P is the normalized pressure value.

Although the interest is that how well 5hrs data fitting follows 100hrs experiment data, squared error of various accumulated data fittings is also calculated to evaluate the pattern of these fits. The data sets used in this part are shown in Table 2.5.

Table 2.5 Data sets evaluated using squared error (real scale)

Data Sets Used for Fitting
5hrs test
10hrs test
20hrs test
50hrs test
100hrs test

Once the squared error is calculated for each case, mean, median and standard deviation of squared error are calculated for 20 cases of 5hrs test and 10 cases of 10hrs and so on. Mean, median and standard deviation values are ranked from 1 to 7 (7 fits in this part), where 7 is appointed to the best fit, 1 to the worst fit and the fits in between accordingly. In filling levels, mean rank is calculated for 4 panels for rank of mean, rank of median and rank of standard deviation. The rank-per-case is also acquired from squared error of each case by using the same ranking method in PPCC test. The results of this part are evaluated considering all four of these rankings. If these values are not in agreement, the median and rank-per-case are given primary importance because mean and standard deviation values are affected significantly by the high values in one single case. In addition, the median and rank-per-case is more important for the reason that, 5hrs sloshing tests are conducted one or two times in the actual procedure. Therefore, each case should return steady estimates for a fit to be considered a good fit.

2.1.5. Estimated Pressure Difference

In the current procedure required by classification societies, 5hrs or 10hrs test data fitting and 3-hour return period is considered in the estimation of maximum pressure. A comparison that is suitable for this procedure is also

carried out. Taking 100hrs experiment data as a reference, summed absolute difference between estimated maximum pressure acquired from fitting and 100hrs experiment data is calculated. For the determination of the experiment data corresponding to 3-hour return period, linear interpolation between pressure values is applied. It was checked that, for 3-hour return period, the data is so close to each other, there is almost no difference between interpolation methods or different curve fitting methods. Once the summed absolute difference of pressures is calculated, mean and rank-per-case of this value is acquired by the same method explained in squared error.

2.2. Peak Pressure Signal Modelling

Peak pressure signals are often idealized as triangular shapes. In the procedure of classification societies and other organizations, two types of signal modelling is currently used (Kim et al., 2014). Type 1 is the triangular shape passing through rise and decay times at the pressure threshold and the maximum pressure P_{max} (Fig. 2.1).

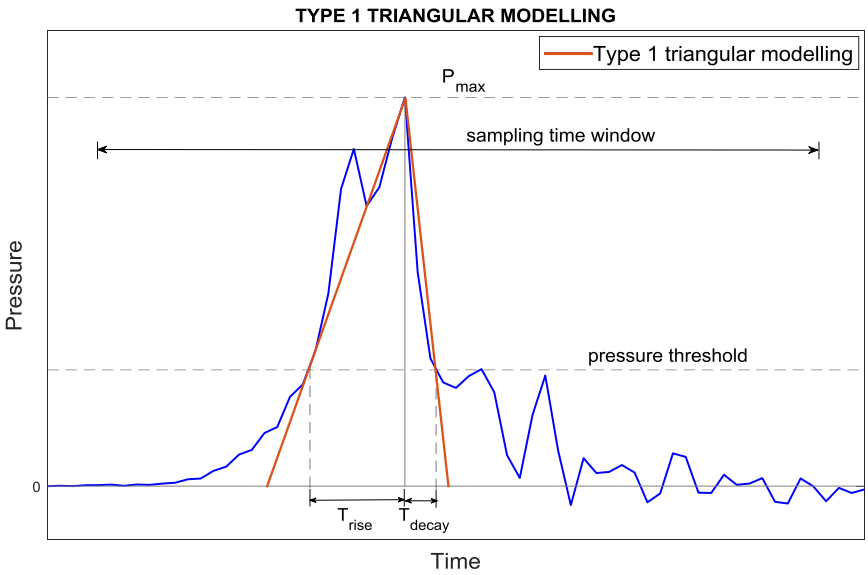

Fig. 2.1 Type 1 triangular modelling applied to peak signals

Type 2 modelling is the triangular shape passing through rise and decay times at a certain ratio of peak pressure and the maximum pressure P_{max} (Fig. 2.2).

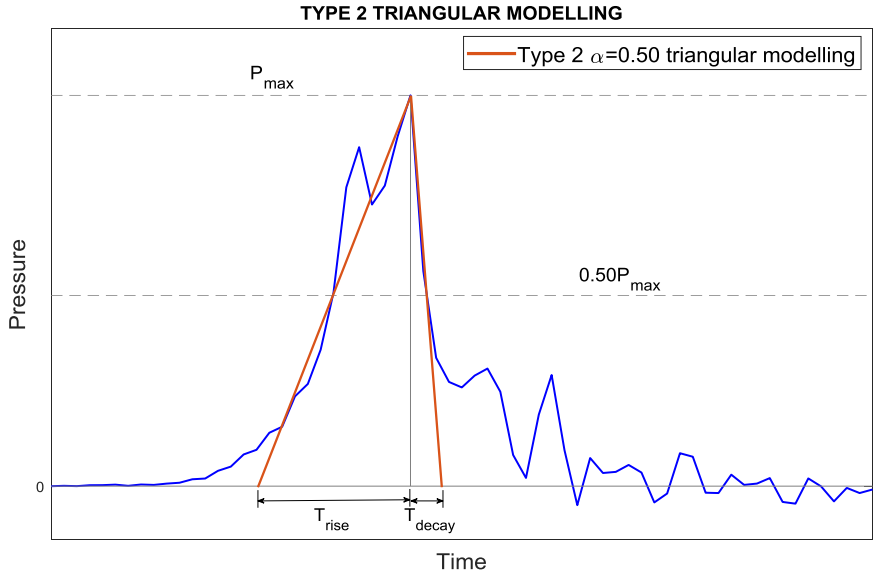

Fig. 2.2 Type 2 triangular modelling applied to peak signals

The formulation of Type 1 and Type 2 modelling methods are given as follows (Kim et al., 2014).

- Type 1:

$$T_{\text{rise}} = t_{P_{\max}} - t_{P_{\text{threshold}}\text{up-crossing}} \tag{50}$$

$$T_{\text{decay}} = t_{P_{\text{threshold}}\text{down-crossing}} - t_{P_{\max}} \tag{51}$$

- Type 2:

$$T_{\text{rise}} = \frac{t_{P_{\max}} - t_{(\alpha_{\text{rise}}.P_{\max})\text{up-crossing}}}{1-\alpha_{\text{rise}}} \tag{52}$$

$$T_{\text{decay}} = \frac{t_{(\alpha_{\text{decay}}.P_{\max})\text{down-crossing}} - t_{P_{\max}}}{1-\alpha_{\text{decay}}} \tag{53}$$

$$\mathrm{T}_{\text{total}} = \mathrm{T}_{\text{rise}} + \mathrm{T}_{\text{decay}} \tag{54}$$

The methods that are currently used in different organizations are shown in Table 2.6. It is seen that, Type 2 modelling and pressure ratio of 0.5 is mostly used.

Table 2.6 Current modelling methods in test facilities and classification societies (Kim et al., 2014)

Organization	**Rise Time**	**Decay Time**
ABS	Type 2 (α=0.5)	Type 2 (α=0.5)
DNV	Type 1 & Type 2 (α=0.5)	Type 1 & Type 2 (α=0.5)
LR	Type 2 (α=0.5)	Type 2 (α=0.5)
BV	Type 2 (α=0.5)	Type 2 (α=0.5)
GTT	Type 2 (α=0.5)	Type 2 (α=0.5)
MARINTEK	Type 2 (α=0.2)	Type 2 (α=0.3)

In this part, pressure ratios for Type 2 triangular modelling are investigated. The rise and decay times in 9 stations of pressure signals are extracted and utilized in comparison of different pressure ratios (Fig. 2.3).

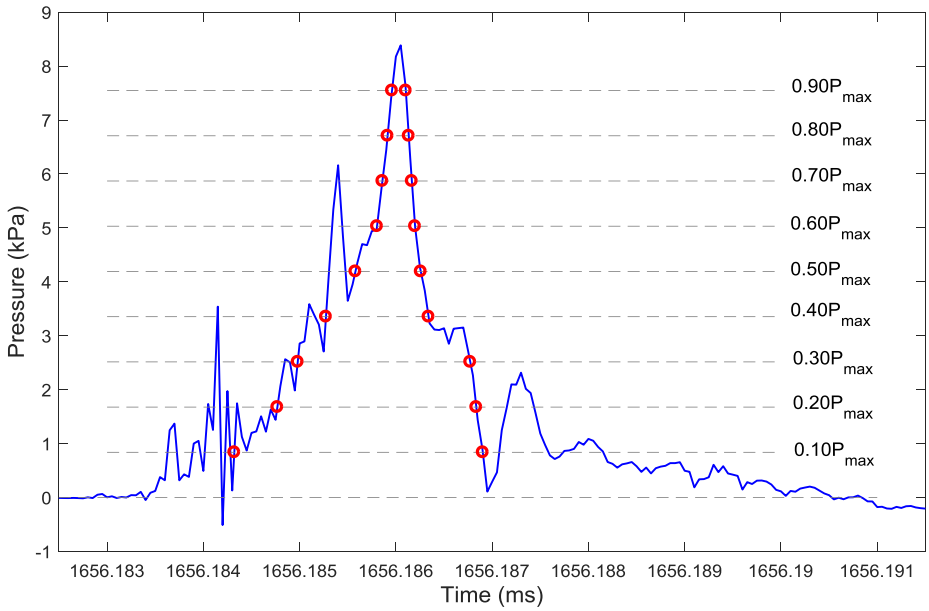

Fig. 2.3 The rise and decay times in 9 stations of P_{max}

To carry out the comparison, the summed absolute difference between the rise and decay times in actual signal and modelled signal is calculated in these 9 stations.

$$\varepsilon_{\text{rise}} = \sum \left| T_{\text{rise,reference}} - T_{\text{rise},(\alpha . P_{\max})} \right| \tag{55}$$

$$\varepsilon_{\text{decay}} = \sum \left| T_{\text{decay,reference}} - T_{\text{decay},(\alpha . P_{\max})} \right| \tag{56}$$

The comparison of pressure ratios is displayed in different percentages of highest peak pressures in each filling level. The comparison is done this way, because pressure signals may show a change of pattern according to pressure values and filling levels. Considering the results, a suggestion is made for pressure ratio of triangular signal modelling.

3. Sloshing Experiment

The tests were conducted in Seoul National University (SNU) Sloshing Experiment Facility. SNU has three hexapod motion platforms with different payloads (1.5, 5, and 14 ton). In this study, 5-ton platform was used with a tank which has 868.2 mm length (L), 760 mm width (B) and 556 mm height (H). A motion platform, which as controlled by a motion controller, was used to simulate the scaled 6-degree of freedom (dof) ship motion. Froude scaling is used. In the experiment, 20 repetitions of 5hrs test (real scale) were carried out in extreme wave condition. The test conditions are shown in Table 3.1. Experiment setup is shown in Fig. 3.1.

Table 3.1 Sloshing test conditions (real scale)

Case	Filling Depth	Heading Angle	Sea Condition	Test Time	Phase Seed
Case 1	0.95H	150deg	T_z = 9.5s H_s = 12.5m	5hrs * 20	Random seed
Case 2	0.50H	90deg	T_z = 11.5s H_s = 9.5m	5hrs * 20	Random seed
Case 3	0.20H	90deg	T_z = 7.5s H_s = 7.5m	5hrs * 20	Random seed

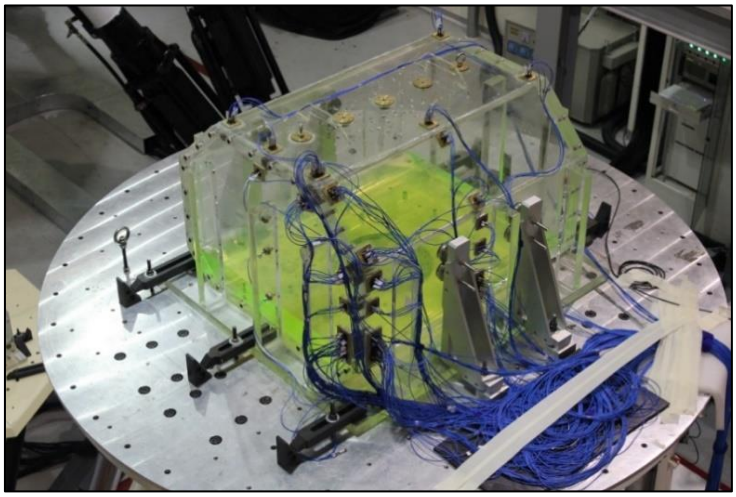

Fig. 3.1 Experiment setup

The tests were conducted for three different filling depths: 20%, 50% and 95% of tank height, notating 0.20H, 0.50H and 0.95H hereafter. The tank is based on 140K Liquefied Natural Gas (LNG) carrier with a 1:50 scale ratio and made of plexiglass. Thickness of the tank is 35-40 mm which is firm enough to regard the wall as rigid and ignore hydroelastic response of the tank. To measure the dynamic pressures on the tank, integrated circuit piezoelectric (ICP) sensors were mounted as cluster panels. There are 24 panels in total and their locations are shown in Fig. 3.2.

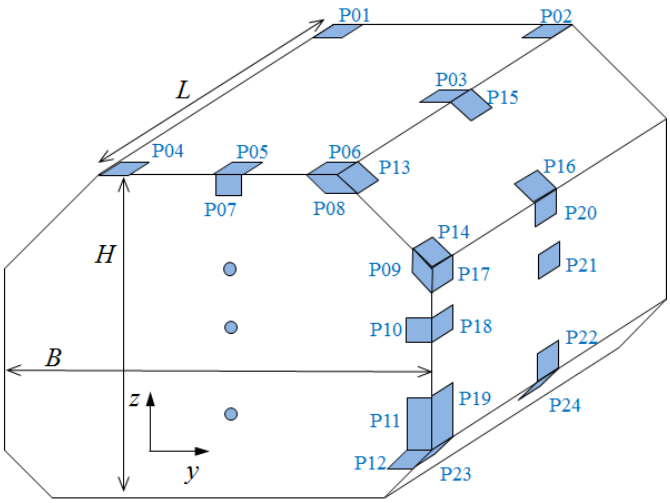

Fig. 3.2 LNGC tank model and location of sensor cluster panels.

Once the pressure data is measured, high-pass filter is used to eliminate low-frequency drift of pressure data. Sampled sloshing peaks, or global peaks, were chosen by imposing pressure threshold (2.5kPa) and sampling time window (0.2ms) (Kim et al. 2017). The maximum pressures collected from all the segments became a group of peaks for the statistical analysis. The panels considered in this study are shown in each filling level in Table 3.2 and the most important panels are underlined. Panels where the highest peak pressures and the most peak pressures occur are chosen for each filling level as these panels are considered to be critical.

Table 3.2 The panels that are considered in this study.

	0.20H	**0.50H**	**0.95H**
PANEL NO.	14	4	1
	19	6	2
	22	14	4
	23	16	6

4. Results & Discussion

4.1. Short Duration Test

Parameter estimation of each distribution is made for peak pressure data acquired from 4 different panels in each filling level. 5hrs test is considered as one case and distributions are fitted to the data of each case for 20 cases. For each fit, probability of exceedance curves are obtained and PPCC test is applied. The results are compared in each filling level separately, because each filling level is expected to have a different pattern of peak pressures distribution.

4.1.1. Statistical Distributions for the First Step

In Fig. 4.1, a sample probability of exceedance diagram of the distributions considered in the first step of this study is shown. 11 distributions are fitted in total and results are compared by observing probability of exceedance diagrams and PPCC tests of many cases. The best 4 distributions are chosen to be Weibull, generalized Pareto, generalized extreme value and log-logistic distributions. These distributions are taken for further study and different distribution fitting methods are applied.

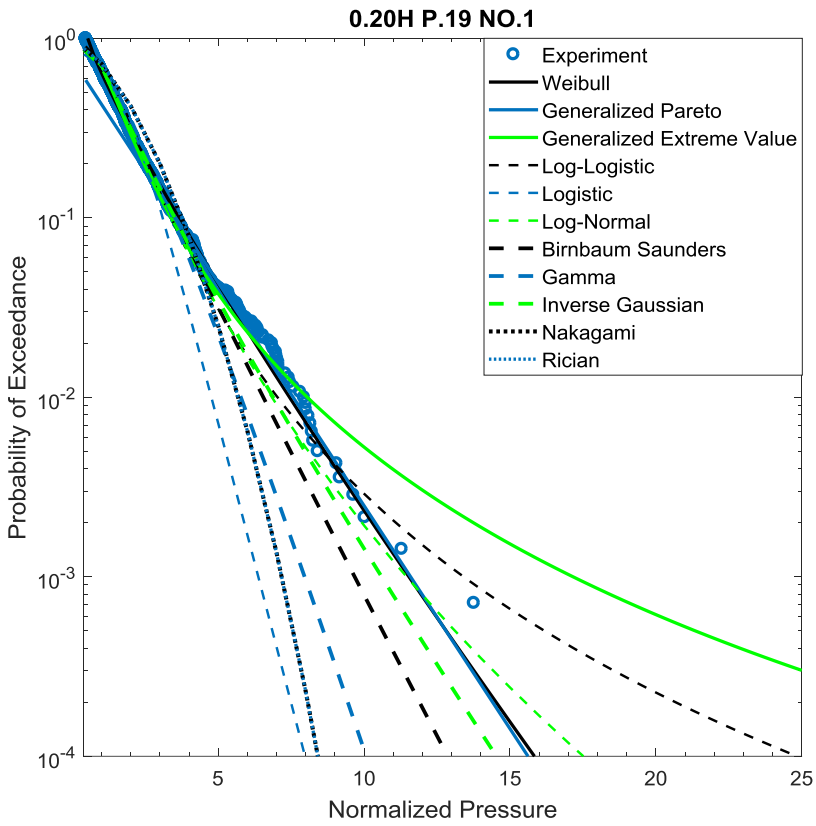

Fig. 4.1 Probability of exceedance diagrams of distributions considered in the first step

4.1.2. PPCC Hypothesis Testing Results

An example of probability exceedance diagrams and PPCC test results are shown in Fig. 4.2 and Table 4.1, respectively. In the figure, 5hrs test data from test number 05 in 20% filling level in panel number 19 is shown as (0.20H, P.19, No.5). This notation will be used hereafter when referring to data sets. A rough comparison between POE curves and PPCC values can be made. First of all, GEV-MLE and LL-MLE fits are obviously poor fits and PPCC values are also lower. When other fits are checked, it is seen that POE curves and PPCC values are roughly in accordance. From PPCC critical values and hypothesis testing results, it is observed that, as the

fits get better, the critical value tends to get larger, which also increases the chance of rejection and vice versa. Taking GEV-MLE as an example, even if PPCC value is low, it was not rejected because critical value is even lower.

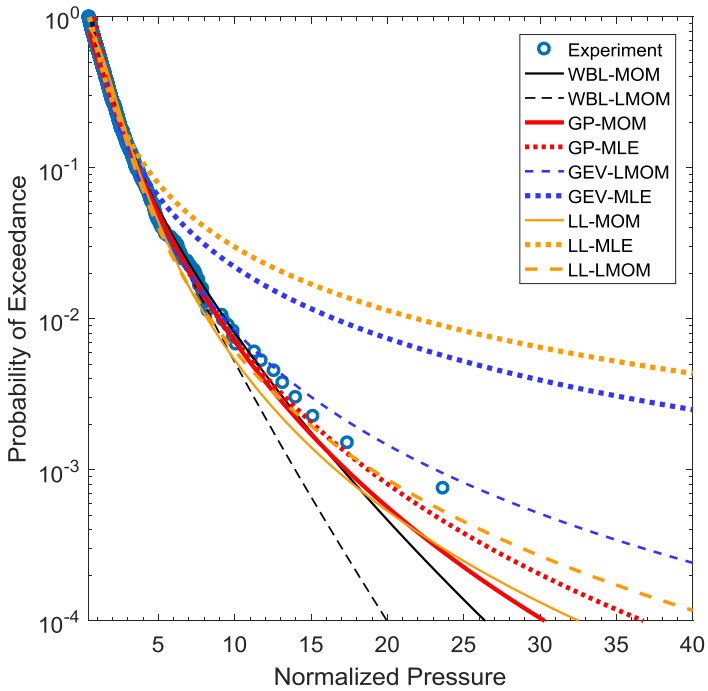

Fig. 4.2 An example of POE diagrams (0.20H P.19 No.05)

Table 4.1 An example of PPCC test results (0.20H P.19 No.05)

Distribution	**PPCC Value**	**PPCC Critical Value**	**Hypothesis Testing**
GP-MLE	0.9993	0.9980	0
GP-MOM	0.9970	0.9987	1
WBL-MOM	0.9953	0.9809	0
GEV-LMOM	0.9941	0.8904	0
LL-LMOM	0.9930	0.9072	0
WBL-LMOM	0.9874	0.9905	1
LL-MOM	0.9853	0.9508	0
GEV-MLE	0.8909	0.8258	0
LL-MLE	0.8107	0.8245	1

PPCC hypothesis testing results are displayed in Fig 4.3. The figure shows the hypothesis test acceptance ratio of each fit in all 3 filling levels. The hypothesis testing uses the critical value obtained from random sampling in a certain significance level and is useful when there is no other reference to compare the PPCC value at hand. However, in this case, the aim is to compare different fits to each other. Therefore, it is difficult to set hypothesis testing as a reference to compare different fits.

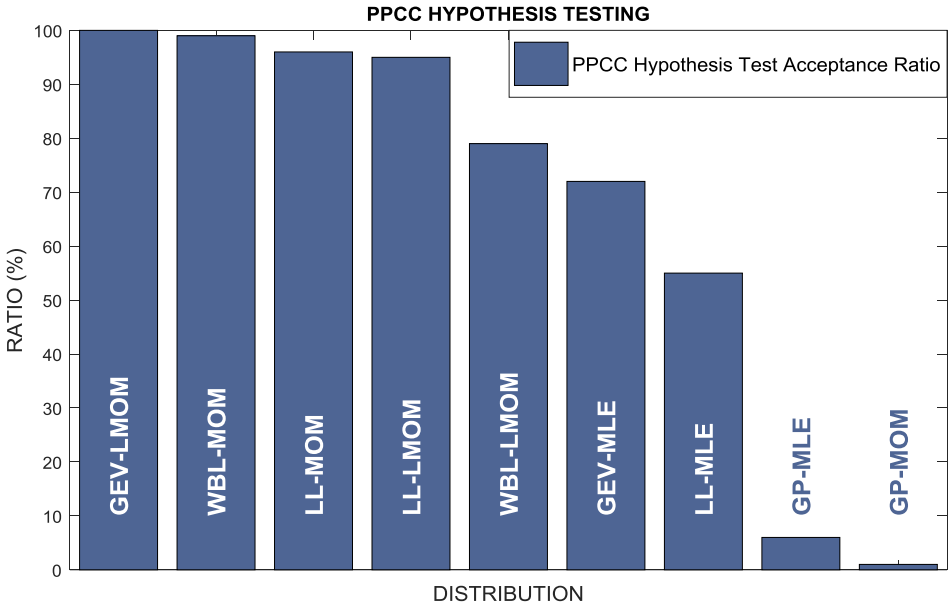

Fig. 4.3 PPCC Hypothesis Test Results

4.1.3. Short Duration PPCC Test Results

Some examples of POE curves are shown in Fig. 4.4. This figure shows representative cases for each filling level, where higher peak pressures mostly occur. The behavior of each distribution can be observed. It can be concluded from these diagrams that GEV-MLE and LL-MLE are poor fits for the data at hand and also, WBL-LMOM does not follow the tail of the distribution as well as other fits. In addition, GP-MLE follows the tail of the

data better than GP-MOM fit. For the reason, GP-MLE does not follow the lower tail, where the smaller pressure values are, as well as GP-MOM. This result can be discussed because it can mean GP-MLE is affected heavily by the highest pressure values and possibly by outliers as well.

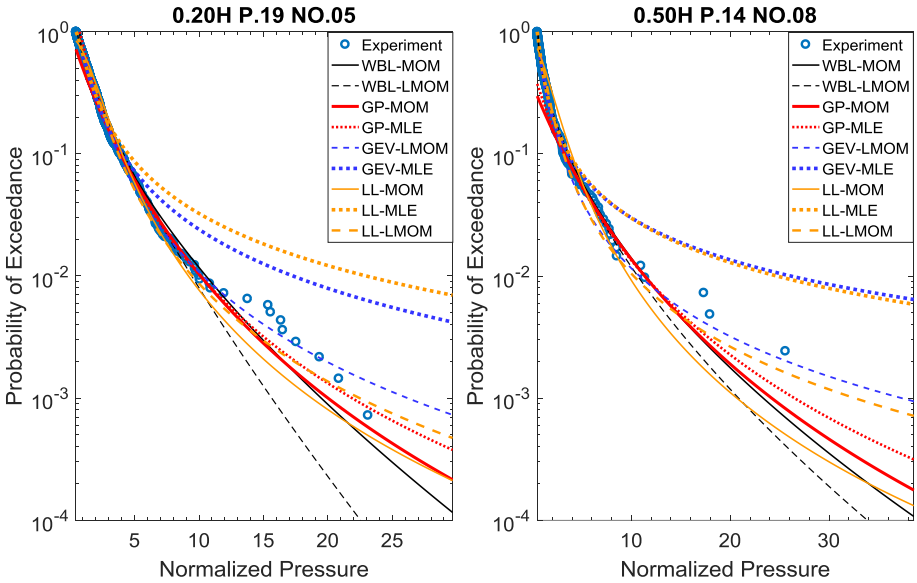

(a) (0.20H P.19 No.05)

(b) (0.50H P.14 No.08)

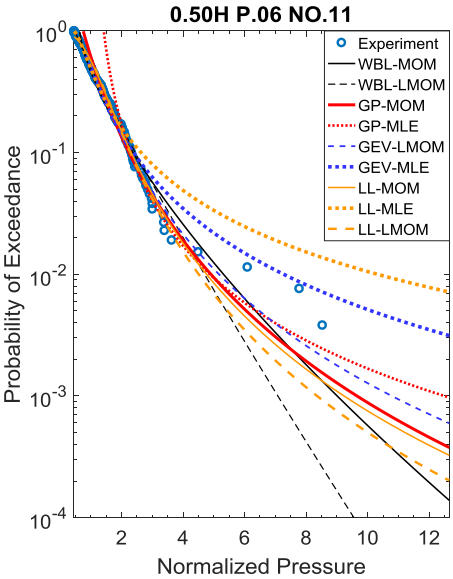

(c) (0.50H P.06 No.11)

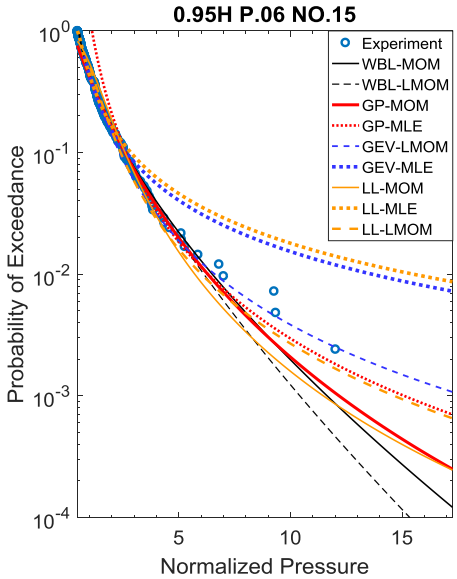

(d) (0.95H P.06 No.15)

Fig. 4.4 Some example POE curves for 5hrs test (real scale)

The PPCC values for each distribution are compared for all filling levels in Fig. 4.5. The distributions are rated according to the ranking method explained in section 3.1.3 and results are displayed in %. When PPCC test results for whole data set is evaluated, WBL gives the highest goodness-of-fit rate in all 3 filling levels. For these two models, MOM provides a better fit than L-MOM method. As expected, GEV-MLE and LL-MLE fits are rated lowest.

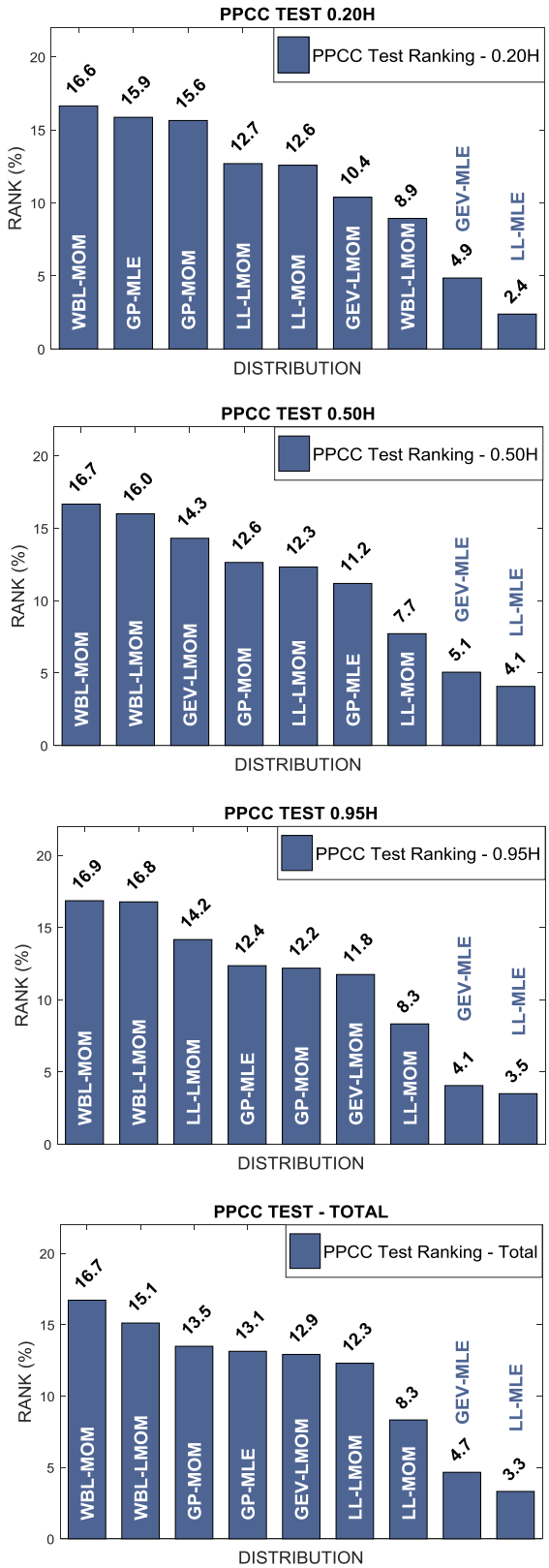

Fig. 4.5 PPCC test results of whole data for 5hrs test (real scale)

However, comparing whole data set fitting to each other can be discussed in several aspects. First, considering the way PPCC is calculated, PPCC test can be sensitive to sample size. In the lower tail (smaller values) of the distribution has a greater number of data while the upper tail (higher values) has a smaller number of data. Therefore, the part of the distribution with higher sample size has a greater affect in PPCC value. This can make a difference when a distribution follows the lower values of the distribution perfectly but provides an upper tail far away from the higher values. It is also arguable to compare GP to other distributions for whole data set. That is because, only 8% highest peaks are considered in each data set for GP fitting and then the parameters for whole data set are obtained. Therefore, most of the time, it is inevitable for GP to be a poor fit for whole data as shown in Fig. 4.6. In hypothesis testing results, it can be observed that the acceptance rate of GP fits is lower than 10%, even though PPCC rates are on the higher side. If the data has extreme peaks in the tail or changes its form significantly in the upper tail when compared to lower tail, GP fit does not follow the whole data. This is the reason why GP hypothesis acceptance rate is low. Moreover, in modelling of peak pressures, the upper tail of the distribution is much more important for the reason that the objective of the distribution fitting is to obtain the maximum pressure value. Considering these, comparing goodness-of-fit test results for whole data is questionable.

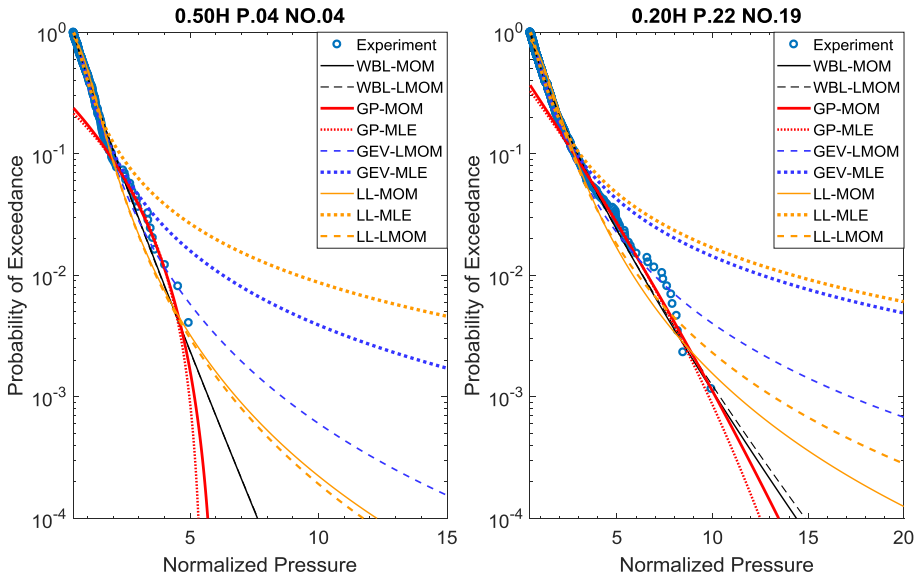

(a) (0.50H P.04 No.04) (b) (0.20H P.22 No.19)

Fig. 4.6 POE diagrams that show the difference of GP fits distinctly.

To overcome these obstacles in evaluating the goodness-of-fit, PPCC test is applied to only 0.92 quantile of the sample peak pressures. PPCC tail-only results for each filling level and for all filling levels are displayed in % in Fig. 4.7 As expected; PPCC test results for tail-only data are more accurate to evaluate the goodness-of fit of the upper tail. It is concluded that WBL-MOM gives the best fit in the tail in 50% and 95% filling levels while GP-MLE is the best fit in 20% filling level followed very closely by LL-MOM and WBL-MOM. The reason why GP-MLE provides better a fit in the tail than the whole data in 20% filling levels is because the cases that the tail has a different pattern than the rest of the data (as in Fig. 4.6) are majority in 20% filling level. On the other hand, WBL-MOM that provides the best fit for whole data does not follow the tail data as well as GP-MLE in 20% filling level. It is also seen that, MLE method is the weakest method for distributions with three parameters.

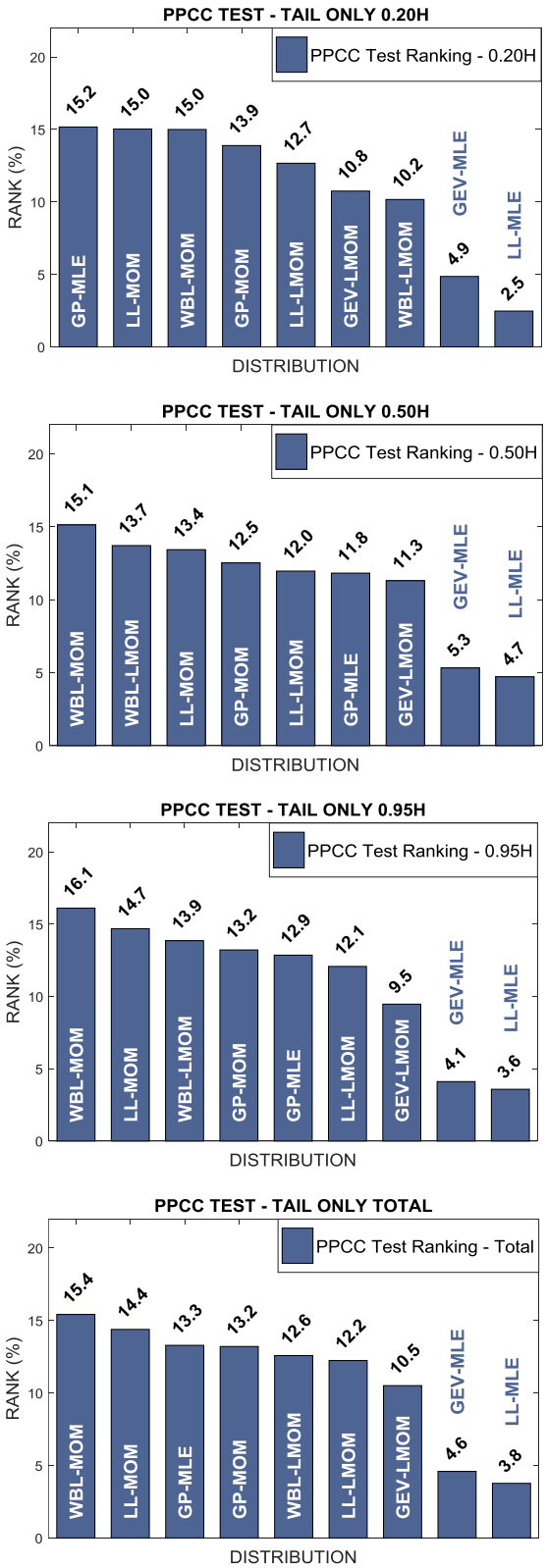

Fig. 4.7 PPCC test results of tail-only data for 5hrs test (%8 highest peaks)

4.2. Long Duration Test

A comparison of long duration test data fitting is also carried out to judge the behavior of fits in longer return periods. Previously mentioned procedure is applied to the accumulated peak pressure data from 20 repetitions of 5hrs test (100hrs, real scale). GEV-MLE and LL-MLE fits are excluded in this part due to poor fits.

4.2.1. Long Duration PPCC Test Results

Example POE diagrams of 5hrs test and 100hrs test data fitting for the same panel are shown in Fig. 4.8. It can be seen that, the pattern of each distribution is similar in both 5hrs and 100hrs test. When pressure values corresponding to 100hrs return period are observed from POE curves of 100hrs test, it is seen that, WBL tends to estimate smaller pressure values compared to GP and LL. While LL returns overestimated values, GP is observed to be consistent. In addition, among the three methods applied in this study, MLE tends to give more conservative curves while MOM results in more conservative fits than L-MOM method in general.

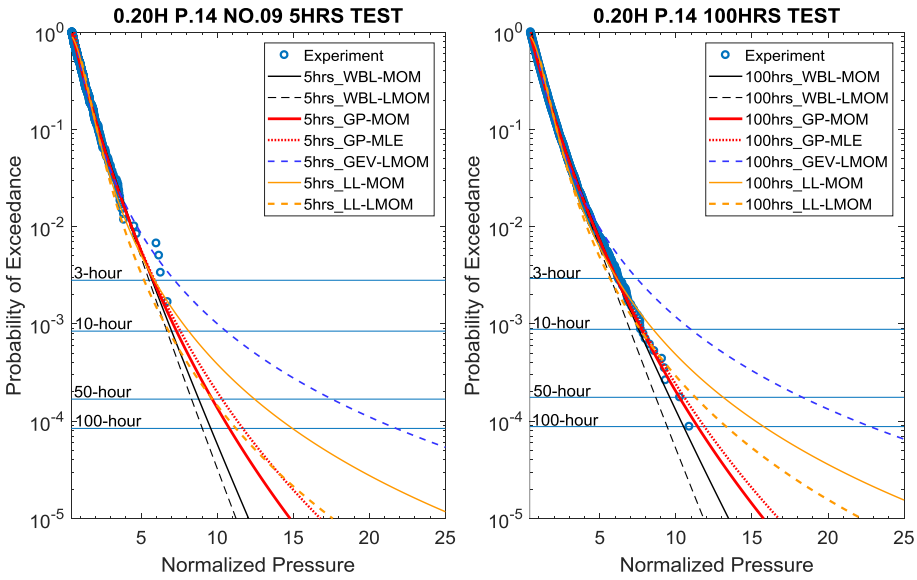

(a) (0.20H P.14)

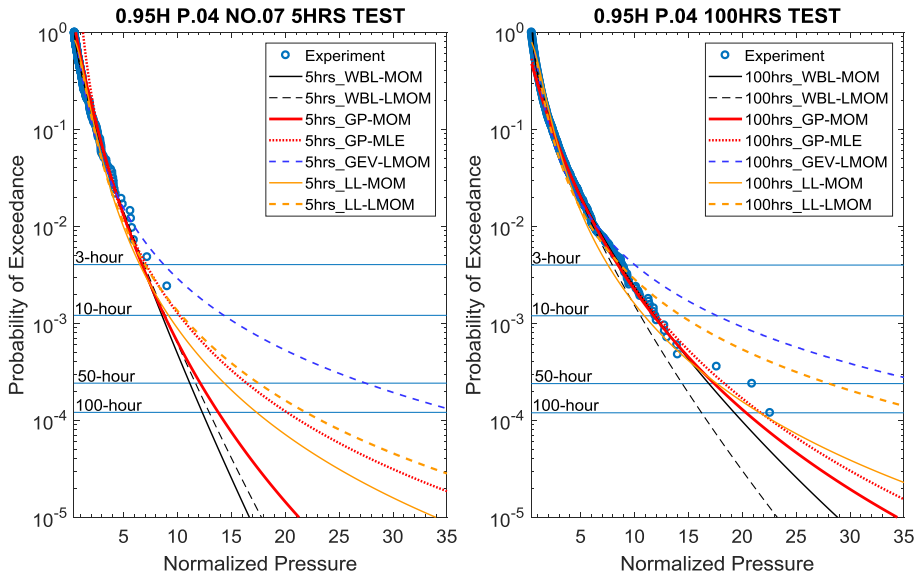

(b) (0.95H P.04)

Fig. 4.8 POE diagrams of 5hrs and 100hrs test (some return periods marked)

PPCC test results of 100hrs test whole data are shown in Fig. 4.9. As concluded from these tables, GP fits provide the best fit in 20% and 50% filling levels while WBL-MOM provides the best fit in 95% filling level.

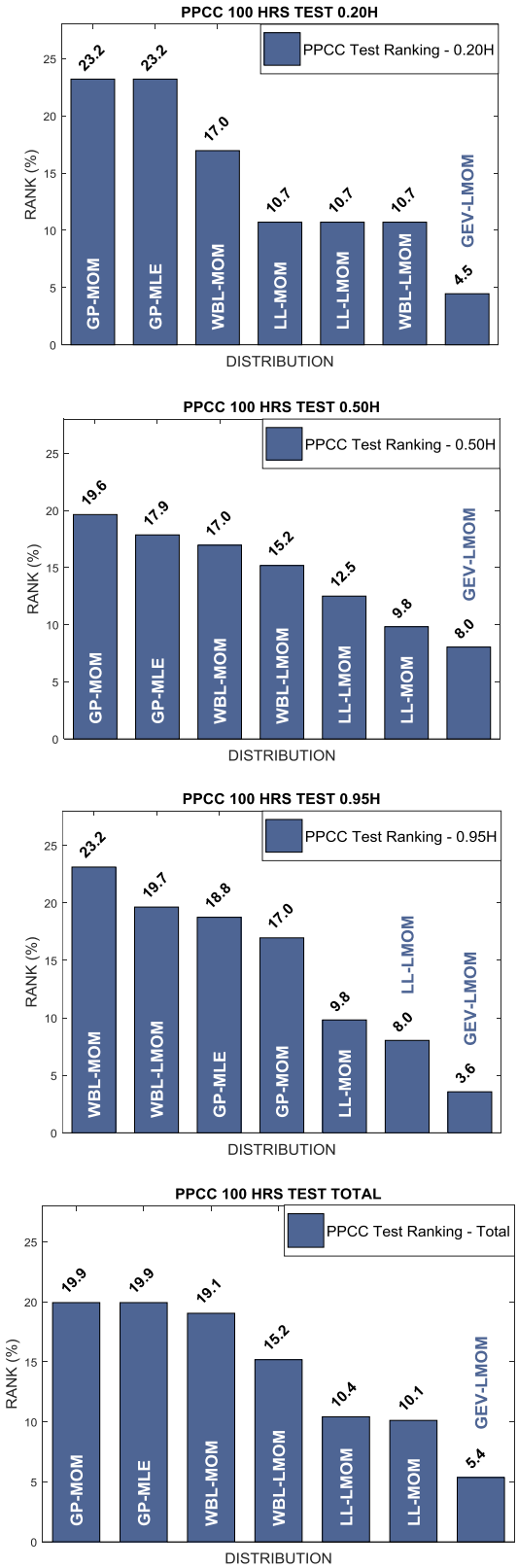

Fig. 4.9 PPCC test results of 100hrs test (real scale) whole data.

PPCC test results of 100hrs test tail-only data are shown in Fig. 4.10. Similar to whole data results, GP fits provide the best fit in 20% and 50% filling levels while WBL-MOM provides the best fit in 95% filling level. The results of whole data and tail-only data are similar, for the reason that, 100hrs test data is more converged and the outliers in the tail are fewer than 5hrs test data. Therefore, the best distributions for each filling levels does not change in tail-only data results in 100hrs test data fitting.

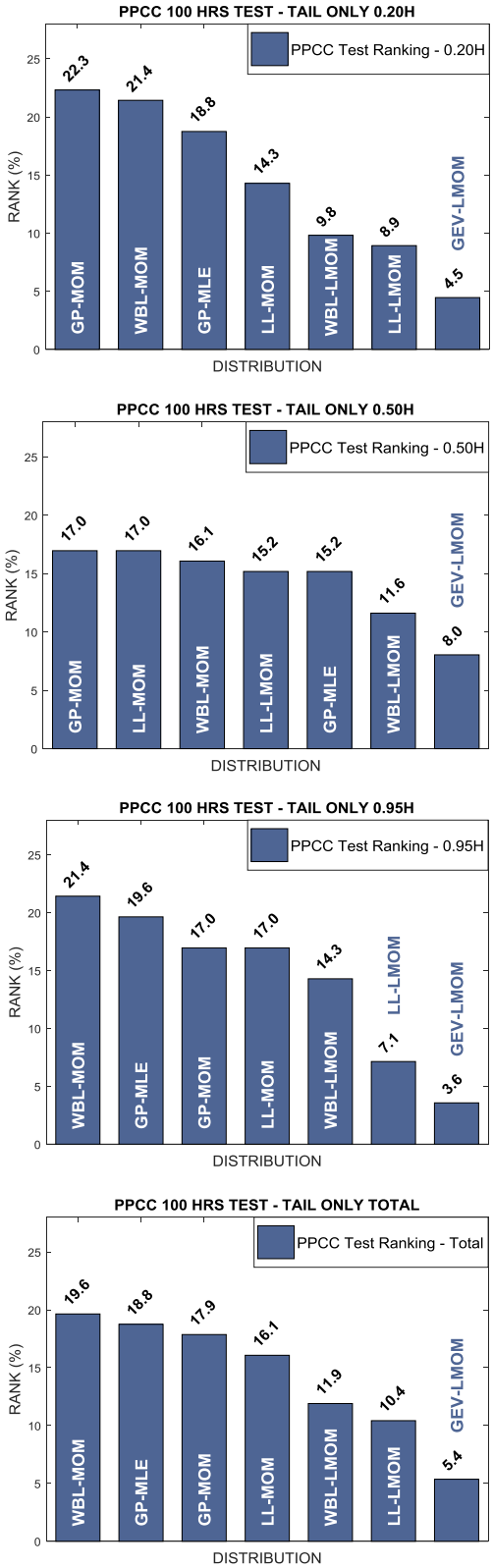

Fig. 4.10 PPCC test results of 100hrs test tail-only data (%8 highest peaks)

4.3. Squared Error Comparison

In this part, squared error between fittings of different data sets and 100hrs experiment data is compared. The comparison is based on mean, median, standard deviation and rank-per-case of squared error. The results are displayed separately for different filling levels, because each filling level is thought to have their own pattern of peak pressures distribution. The results of the most important panels are displayed separately as well, because these panels have the highest and the most number of peak pressures.

4.3.1. Squared Error Comparison According to Filling Levels

The closest fits are displayed in Table 4.2, Table 4.3 and Table 4.4 according to filling levels, data sets and return period zones. In all filling levels, LL-LMOM is the closest fit in Zone 1. Based on 5hrs test data fitting, LL-MOM is the closest fit in Zones 2, 3 and 4 in all filling levels except 50% filling level Zone 2. In 50% filling level, GEV-LMOM is the closest fit in Zone 2. In 50% and 95% filling levels, LL-MOM dominates Zones 3 and 4. It is also seen that GP fits give closest fits in longer return periods when longer duration test data is used. Therefore, it can be concluded that, GP fits provide closer fits when number of data is higher. Although the closest fit changes from one data set to another, a pattern can be seen partially.

Table 4.2 Best fits in each zone compared by squared error in 0.20H

BEST FIT FOR EACH ZONE			
0.20H			
5HRS TEST			
ZONE 1	ZONE 2	ZONE 3	ZONE 4
LL-LMOM	LL-MOM	LL-MOM	LL-MOM
10HRS TEST			
ZONE 1	ZONE 2	ZONE 3	ZONE 4
LL-LMOM	LL-MOM	LL-MOM	GP-MOM
20HRS TEST			
ZONE 1	ZONE 2	ZONE 3	ZONE 4
LL-LMOM	LL-MOM	LL-LMOM	GP-MOM
50HRS TEST			
ZONE 1	ZONE 2	ZONE 3	ZONE 4
LL-LMOM	LL-MOM	LL-LMOM	GP-MOM
100HRS TEST			
ZONE 1	ZONE 2	ZONE 3	ZONE 4
LL-LMOM	LL-LMOM	LL-LMOM	GP-MOM

Table 4.3 Best fits in each zone compared by squared error in 0.50H

BEST FIT FOR EACH ZONE			
0.50H			
5HRS TEST			
ZONE 1	ZONE 2	ZONE 3	ZONE 4
LL-LMOM	GEV-LMOM	LL-MOM	LL-MOM
10HRS TEST			
ZONE 1	ZONE 2	ZONE 3	ZONE 4
LL-LMOM	GEV-LMOM	LL-MOM	LL-MOM
20HRS TEST			
ZONE 1	ZONE 2	ZONE 3	ZONE 4
LL-LMOM	GEV-LMOM LL-MOM	LL-MOM	LL-MOM
50HRS TEST			
ZONE 1	ZONE 2	ZONE 3	ZONE 4
LL-LMOM	GEV-LMOM	GP-MLE GP-MOM	LL-MOM
100HRS TEST			
ZONE 1	ZONE 2	ZONE 3	ZONE 4
LL-LMOM	LL-MOM	LL-MOM	GP-MOM

Table 4.4 Best fits in each zone compared by squared error in 0.95H

BEST FIT FOR EACH ZONE			
0.95H			
5HRS TEST			
ZONE 1	ZONE 2	ZONE 3	ZONE 4
LL-LMOM	LL-MOM	LL-MOM	LL-MOM
10HRS TEST			
ZONE 1	ZONE 2	ZONE 3	ZONE 4
LL-LMOM	LL-MOM	LL-MOM	LL-MOM
20HRS TEST			
ZONE 1	ZONE 2	ZONE 3	ZONE 4
LL-LMOM	LL-MOM	LL-MOM	LL-MOM
50HRS TEST			
ZONE 1	ZONE 2	ZONE 3	ZONE 4
LL-LMOM	GP-MLE LL-MOM	GP-MLE	LL-MOM
100HRS TEST			
ZONE 1	ZONE 2	ZONE 3	ZONE 4
LL-LMOM	LL-MOM GP-MOM GP-MLE	LL-MOM	GP-MOM

4.3.2. Squared Error Comparison in Important Panels

The closest fits in 20% filling level panel 19 are displayed in Table 4.5 according to data sets and return period zones. In this panel, Zone 1 is dominated by LL-MOM and Zone 4 is dominated by GP-MOM regardless of the data set. Based on 5hrs test data, LL-MOM is the closest fit in Zones 2 and 3 similar to 20% filling level results.

Table 4.5 Best fits in each zone compared by squared error in 0.20H P.19

BEST FIT FOR EACH ZONE			
0.20H P.19			
5HRS TEST			
ZONE 1	ZONE 2	ZONE 3	ZONE 4
LL-LMOM	LL-MOM	LL-MOM	GP-MOM
10HRS TEST			
ZONE 1	ZONE 2	ZONE 3	ZONE 4
LL-LMOM	LL-LMOM	LL-MOM	GP-MOM
20HRS TEST			
ZONE 1	ZONE 2	ZONE 3	ZONE 4
LL-LMOM	LL-LMOM	LL-MOM GP-MLE	GP-MOM
50HRS TEST			
ZONE 1	ZONE 2	ZONE 3	ZONE 4
LL-LMOM	LL-LMOM GP-MLE	GP-MLE	GP-MOM
100HRS TEST			
ZONE 1	ZONE 2	ZONE 3	ZONE 4
LL-LMOM	LL-LMOM	GP-MLE	GP-MOM

In order to have a better understanding of this result, 5hrs test data fitting for 20 cases are plotted on 100hrs experiment data for this panel as shown in Fig. 4.11. Each diagram belongs to one of the fits. As seen in the diagrams, WBL-MOM provides a poor fit and it underestimates the maximum pressure in all of the cases. GP-MOM fit matches well with the data corresponding to longer return period in accordance with the squared error results. It is also understood that WBL-MOM, GP-MOM and GP-MLE fits have a larger deviation than GEV-LMOM, LL-MOM and LL-LMOM fits. This deviation is important because a steady estimation of maximum pressure is needed for each case. Between GEV-LMOM and LL-MOM fits, which show small deviation, LL-MOM returns estimates closer to the experiment data in general, also in agreement with the squared error results.

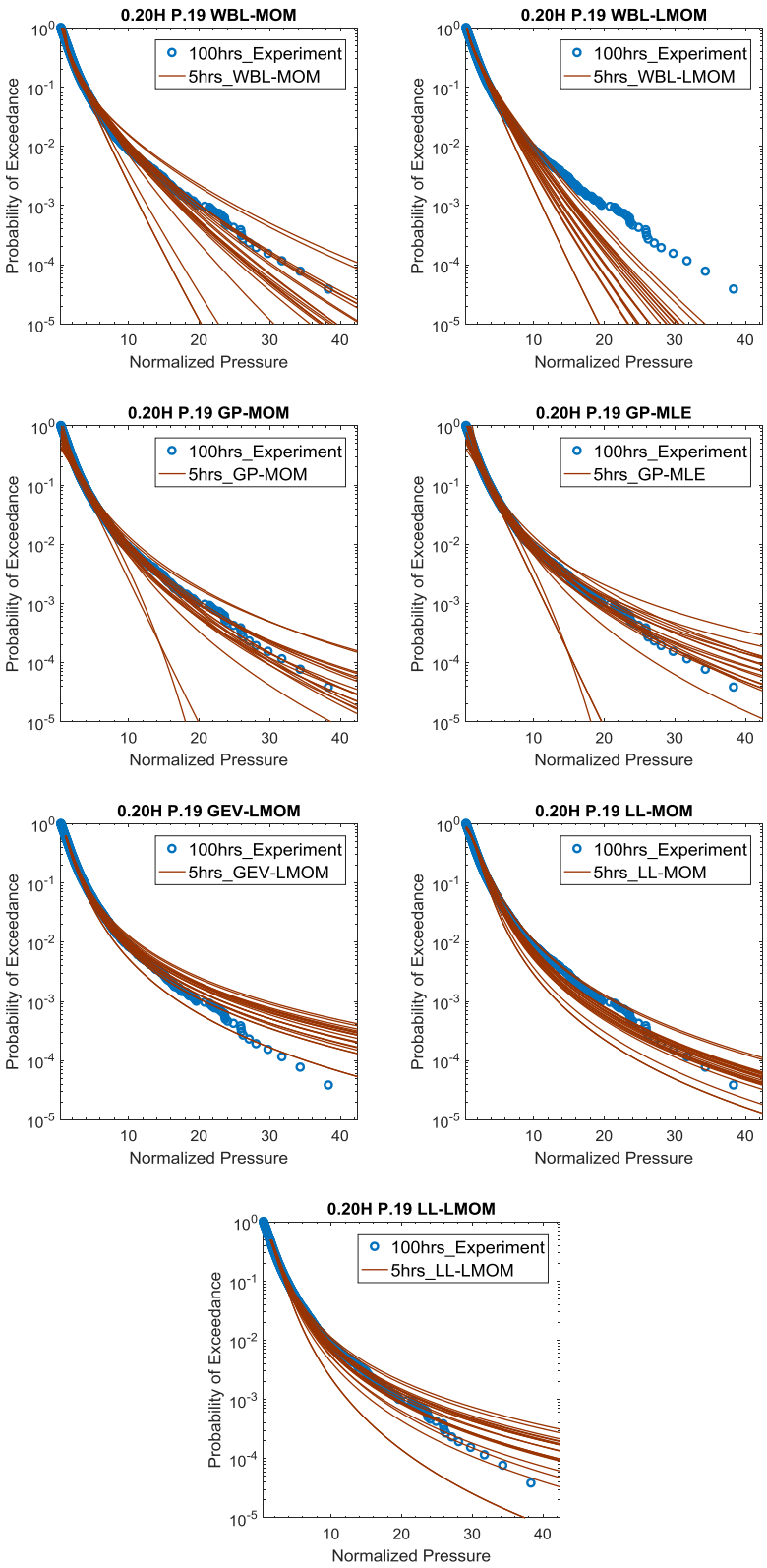

Fig. 4.11 Long term plotting of 5hrs test (real scale) in 0.20H P.19

The closest fits in 50% filling level panel 14 are displayed in Table 4.6 according to data sets and return period zones. In this panel, Zone 1 is dominated by LL-MOM, similar to 20% filling level results. For longer duration test, Zones 2, 3 and 4 are dominated by GP fits. Based on 5hrs test data, GEV-LMOM provides the closest fit in Zone 2 while LL-MOM provides the closest fit in Zones 3 and 4.

Table 4.6 Best fits in each zone compared by squared error in 0.50H P.14

BEST FIT FOR EACH ZONE			
0.50H P.14			
5HRS TEST			
ZONE 1	ZONE 2	ZONE 3	ZONE 4
LL-LMOM	GEV-LMOM	LL-MOM	LL-MOM
10HRS TEST			
ZONE 1	ZONE 2	ZONE 3	ZONE 4
LL-LMOM	GEV-LMOM	LL-MOM	LL-MOM
	GP-MLE	GP-MOM	
20HRS TEST			
ZONE 1	ZONE 2	ZONE 3	ZONE 4
LL-LMOM	GP-MLE	GP-MOM	WBL-MOM
	GP-MOM		
50HRS TEST			
ZONE 1	ZONE 2	ZONE 3	ZONE 4
LL-LMOM	GP-MLE	GP-MLE	GP-MOM
		GP-MOM	
100HRS TEST			
ZONE 1	ZONE 2	ZONE 3	ZONE 4
LL-LMOM	GP-MLE	GP-MLE	GP-MOM

In this panel, the diagrams of 5hrs test data fitting for 20 cases plotted on 100hrs experiment data are shown in Fig. 4.12. These diagrams show that, WBL and GP fits estimate a wider range of maximum pressures and the estimation differs from case to case significantly. On the other hand, GEV and LL fits have much smaller deviation of curves which leads to steady estimates in each case. Therefore, according to shape of the distribution, GEV-LMOM, LL-MOM and LL-LMOM fits return smaller squared error results in the

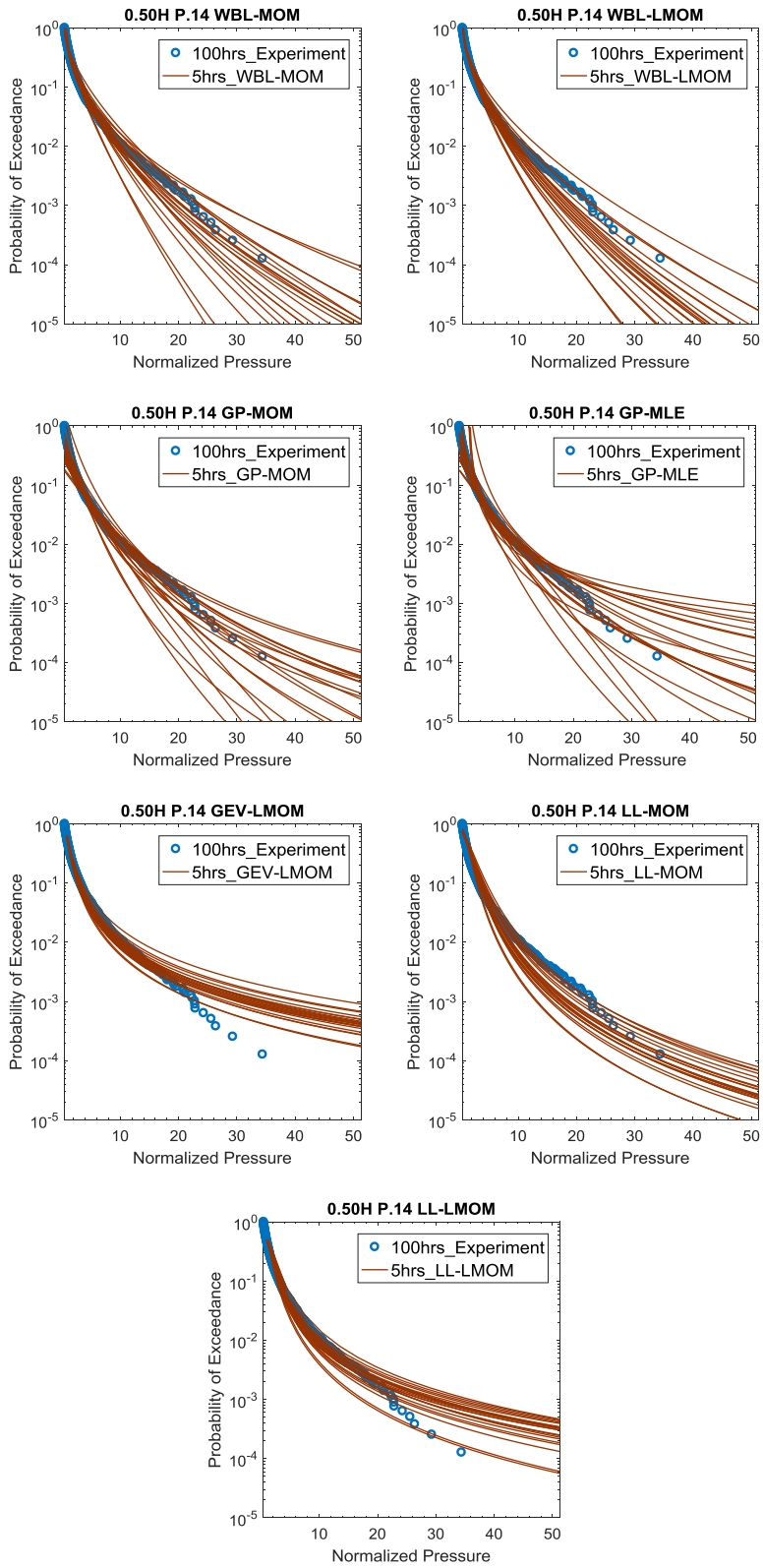

Fig. 4.12 Long term plotting of 5hrs test (real scale) in 0.50H P.19

return period zones where they get closer to the data. This justifies squared error results based on 5hrs test data.

The closest fits in 95% filling level panel 06 are displayed in Table 4.7 according to data sets and return period zones. In this panel, similarly, Zone 1 is dominated by LL-LMOM fit. Based on 5hrs test data, LL-MOM returns the closest fits in Zones 2, 3 and 4. For the longer duration test and longer return periods, a pattern in only seen partially.

Table 4.7 Best fits in each zone compared by squared error in 0.95H P.06

BEST FIT FOR EACH ZONE			
0.95H P.06			
5HRS TEST			
ZONE 1	ZONE 2	ZONE 3	ZONE 4
LL-LMOM	LL-MOM	LL-MOM	LL-MOM
10HRS TEST			
ZONE 1	ZONE 2	ZONE 3	ZONE 4
LL-LMOM	LL-LMOM	LL-MOM	LL-MOM
20HRS TEST			
ZONE 1	ZONE 2	ZONE 3	ZONE 4
LL-LMOM	LL-MOM	WBL-MOM	LL-MOM
50HRS TEST			
ZONE 1	ZONE 2	ZONE 3	ZONE 4
LL-LMOM	LL-MOM	WBL-MOM	GP-MLE
			GP-MOM
		LL-MOM	WBL-MOM
100HRS TEST			
ZONE 1	ZONE 2	ZONE 3	ZONE 4
LL-LMOM	LL-MOM	WBL-MOM	GP-MOM

In this panel, the diagrams of 5hrs test data fitting for 20 cases plotted on 100hrs experiment data are shown in Fig. 4.13. Through the diagrams, it is seen that, WBL and GP fits provide even larger deviation of curves. Especially, GP fits return significantly different values of estimated pressure. One of the possible reasons for this behavior of GP fits would be sample sizes too small. However, comparing to 50% filling level panel 14, which is

previously shown, this panel has much larger sample sizes, yet larger deviation of curves. Therefore, small sample size is not the reason of GP providing this variation of curves. The reason is that, GP follows the tail data so well that it cannot follow 100hrs test data. Similarly, WBL distribution also follows the whole data well and very smoothly and for the same reason, it cannot follow 100hrs test data as well. WBL and GP fits are affected by the data significantly, while GEV and LL fits are affected less and tend to keep their shapes. This way, GEV and LL fits provide a smaller deviation of curves and consistent estimates of maximum pressure. It is obvious that, smaller deviation does not necessarily mean that the fit follows the data well; however, it is convenient to choose the closest distribution among them according to these preserved shapes.

In addition, another long term plotting is shown to evaluate if 1hrs test data fittings have the same pattern as 5hrs test data fittings. In 50% filling level panel 14, the diagrams of 1hrs test data fitting for 30 cases plotted on 100hrs experiment data are shown in Fig. 4.14. It is seen that, deviation is larger for every fit which is an expected result of 1hrs test data fitting. Even if it is the case, GEV-LMOM and LL-MOM fits have smaller deviation than WBL and GP fits.

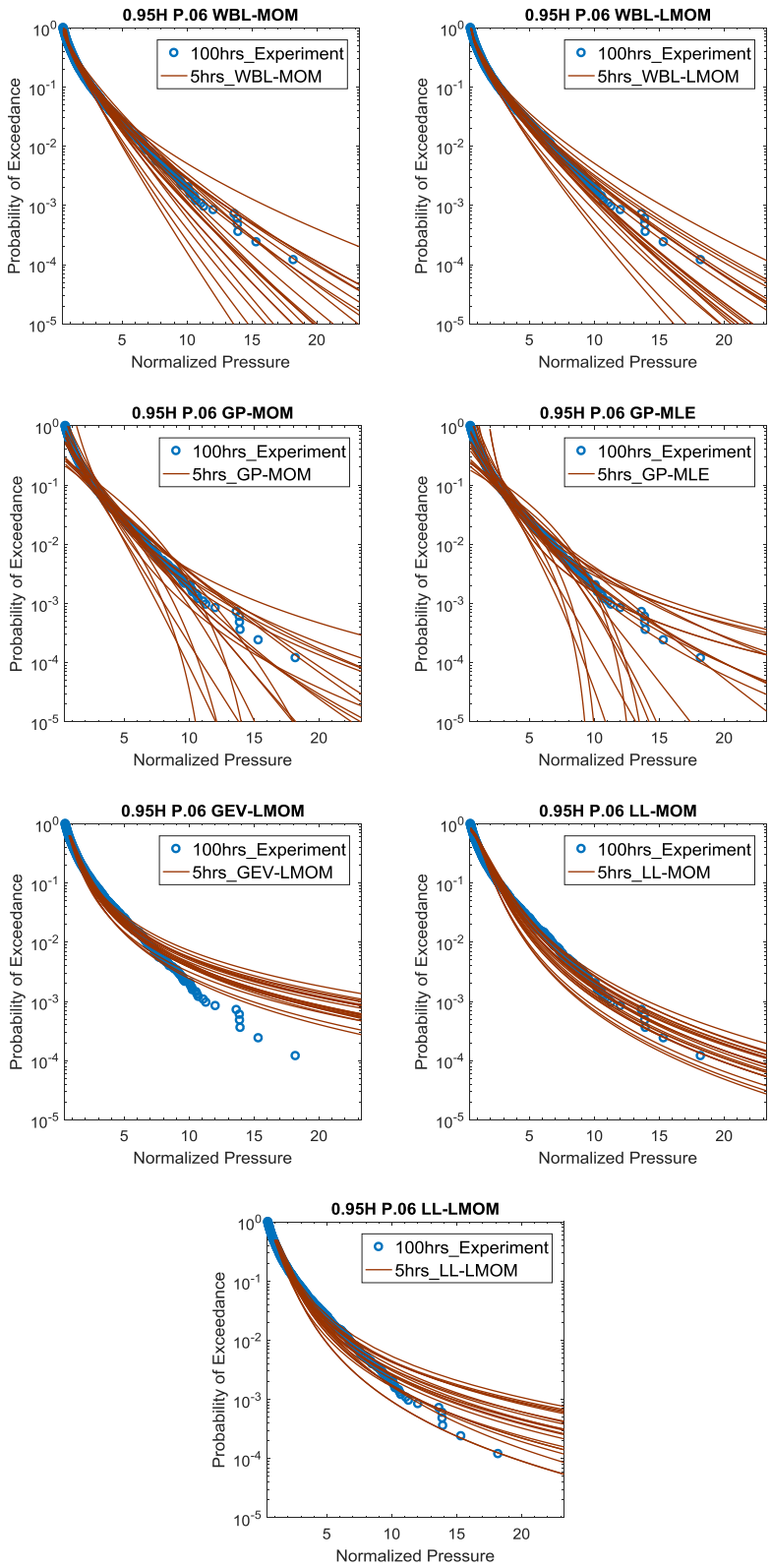

Fig. 4.13 Long term plotting of 5hrs test (real scale) in 0.95H P.06

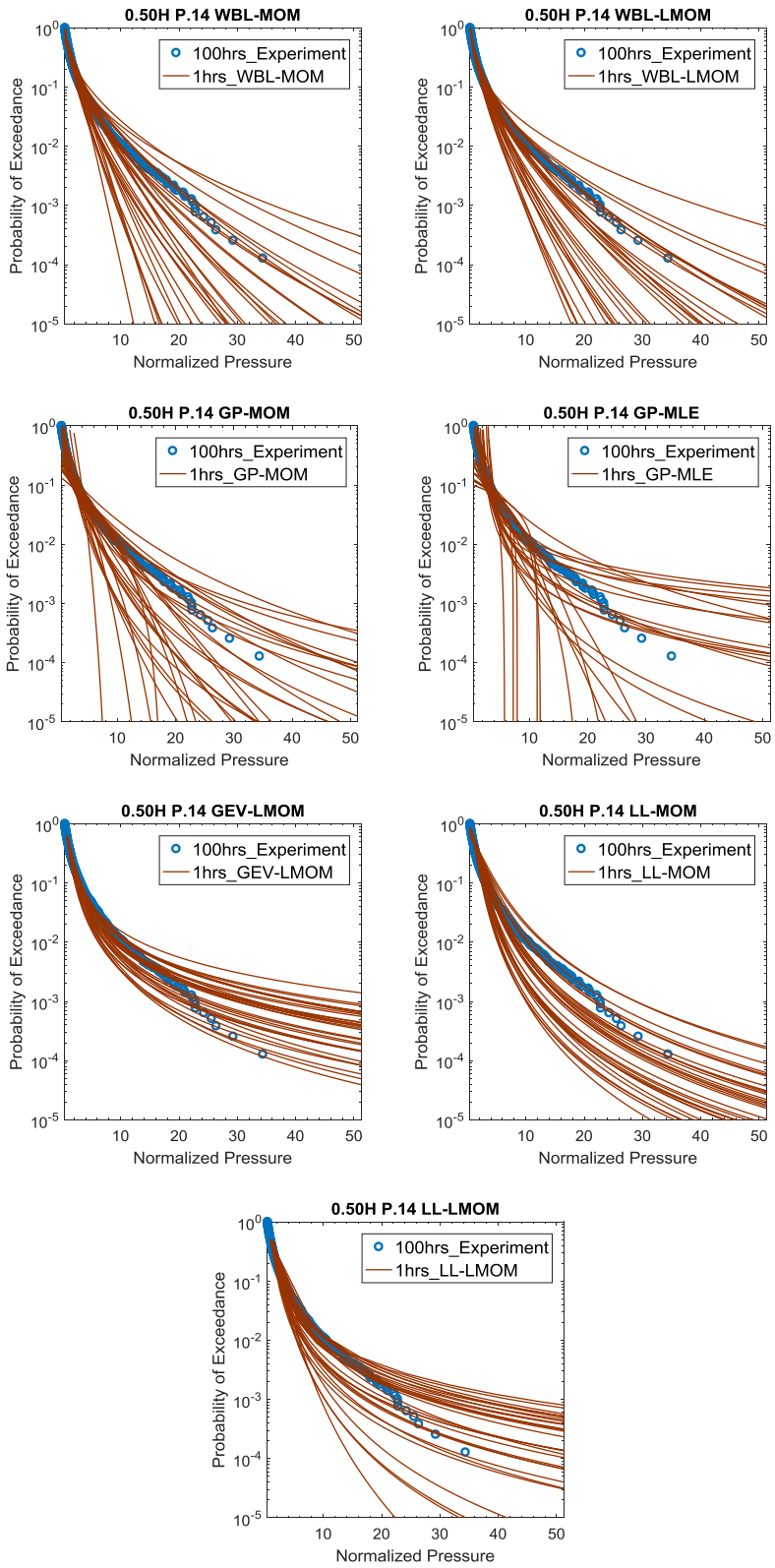

Fig. 4.14 Long term plotting of 1hr test (real scale) in 0.50H P.14

4.4. Estimated Pressure Difference Results

In this part, 100hrs experiment data is taken as a reference and a comparison that is suitable for the current procedure of classification societies is carried out. Summed absolute difference between estimated maximum pressure acquired from 5hrs and 10hrs fittings and 100hrs experiment data is calculated and utilized to make the comparison. The fits that provide the closest fit are shown in Table 4.8 according to filling levels and data sets. For 20% and 95 % filling levels, LL-MOM and for 50% filling level GEV-LMOM provide the closest fits.

Table 4.8 Best fits compared by estimated pressure difference in 3-hour return period.

BEST FIT FOR EACH ZONE (3HR RETURN PERIOD)		
0.20H	**0.50H**	**0.95H**
5HRS TEST		
LL-MOM	GEV-LMOM	LL-MOM
10HRS TEST		
LL-MOM	GEV-LMOM LL-MOM	LL-MOM

4.5. Peak Pressure Signal Modelling Results

In this part, pressure ratios (α) from 0.1 to 0.9 are compared to determine the closest ratio of triangular modelling to the actual signal. The summed absolute difference (ε_{rise}, ε_{decay}) between rise and decay times calculated in 9 stations of pressure signal and the modelled rise and decay times in these stations is compared. The results are displayed according to filling levels and rise and decay times in Fig. 4.15. In these diagrams, the curves represent different ranges of peak pressure numbers in important

panels of each filling level. 90-100% PP indicates the lowest 10% of peak pressures and 0-10% PP indicates the highest 10% of peak pressures in that specific filling level or panel. The comparison is done this way, because pressure signals may show a change of pattern according to pressure value and filling levels. It is concluded from the diagrams that 0.3 is the closest pressure ratio in all three panels for both rise and decay time.

The comparison results are shown in Fig. 4.16 according to different filling levels. It can be seen that, 0.30 is the closest pressure ratio in all three filling levels rise and decay times except 20% filling level decay time. 20% filling level decay time has no obvious pattern. It is observed that, the rising pressure signals usually have a very similar pattern and a clean rise until peak value without irregularities. Hence, the result for rise times is an expected result. However, decaying pressure signals usually contain local peaks, are very irregular and difficult to classify. Therefore, 50% and 95% decay times having an obvious pattern is an unexpected result given these irregularities.

The pattern of the highest values of peak pressure is another subject of interest. Therefore, comparison for 1% to 5% highest peak pressures of each filling level is also carried out and displayed in Fig. 4.17 according to filling levels, rise and decay time. Similar to the previous results, 0.3 is the closest pressure ratio in all three filling level rise and decay times in these particular ratios (0.1~0.5%) of highest peak pressures.

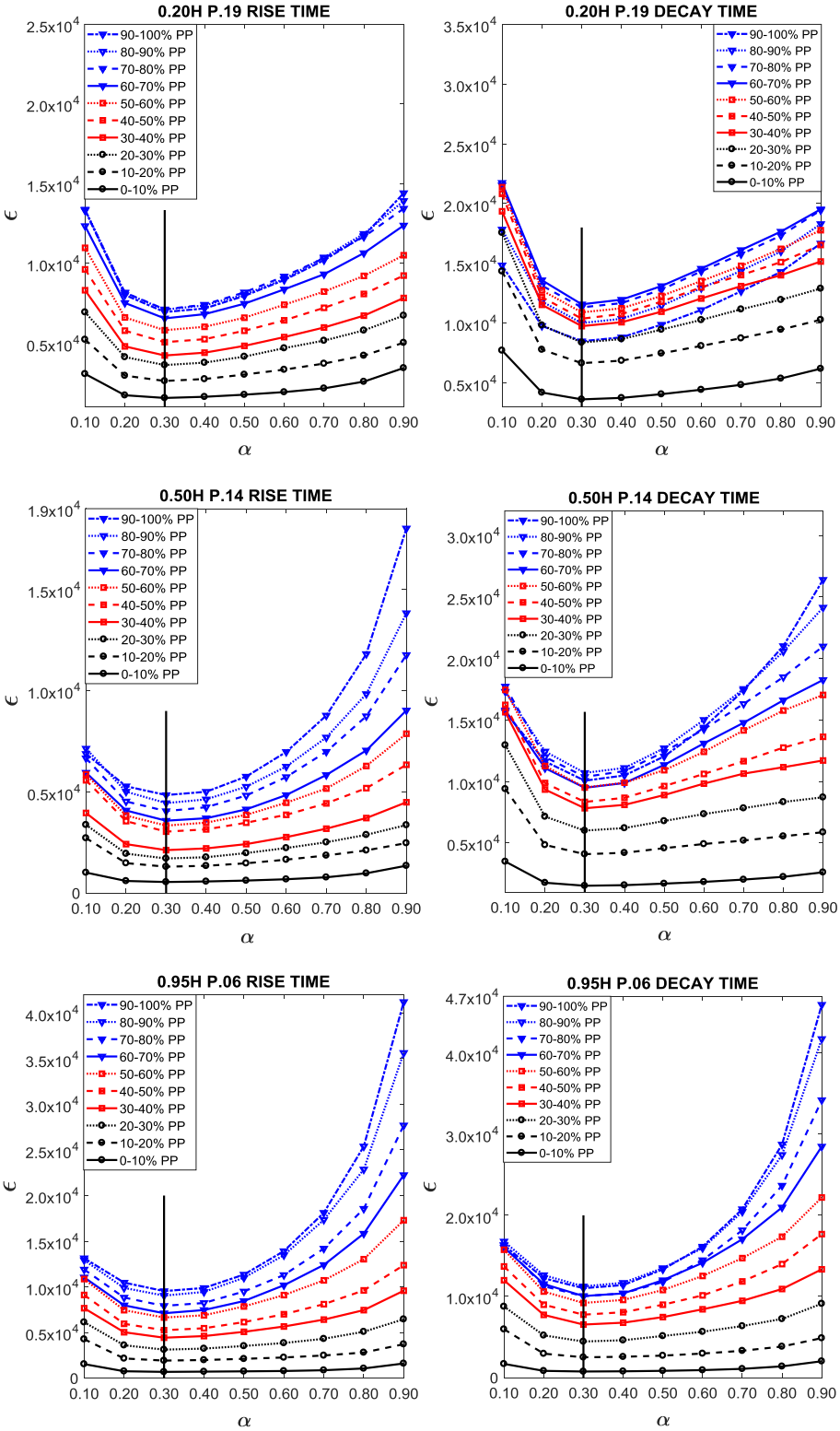

Fig. 4.15 Summed absolute pressure difference in chosen panels.

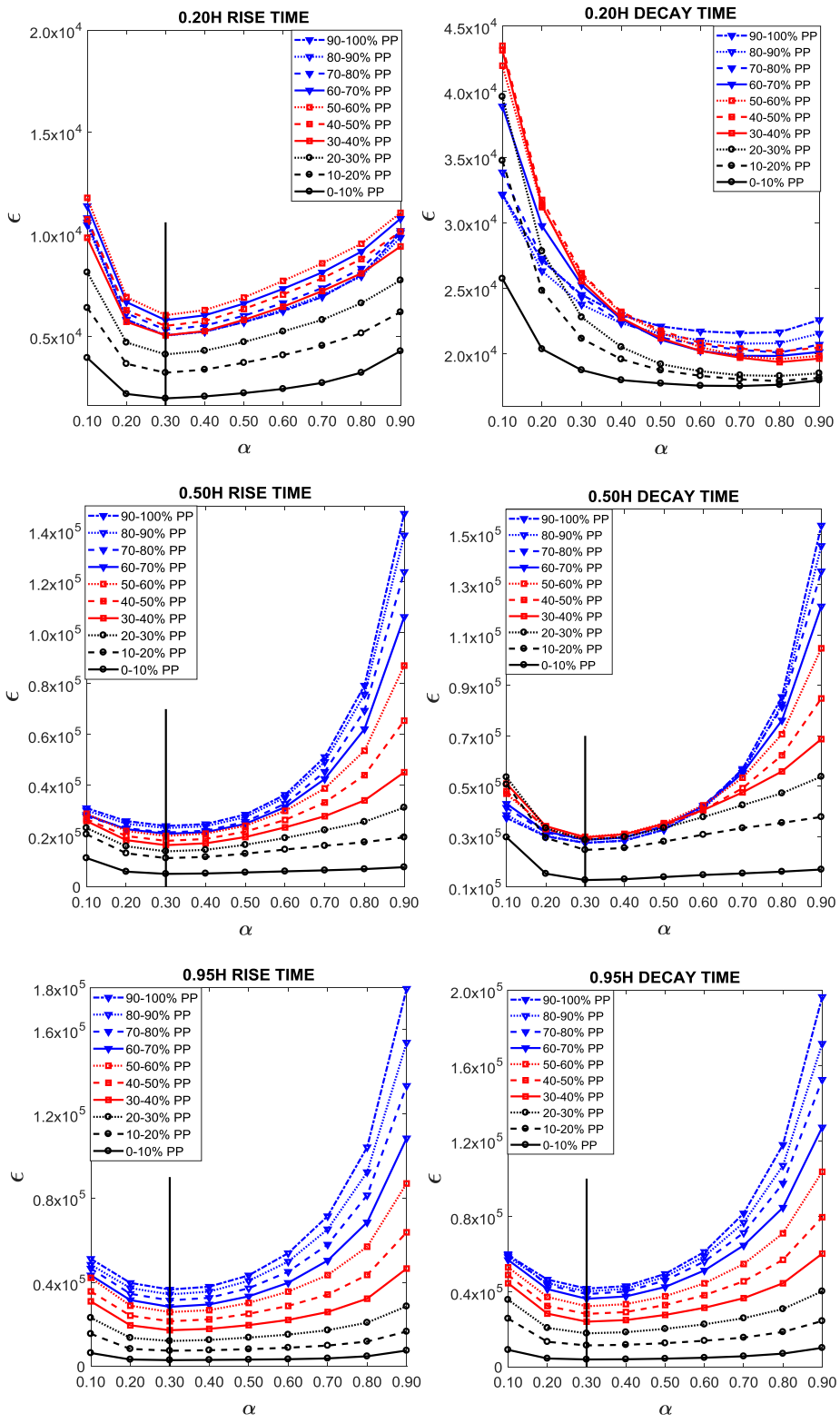

Fig. 4.16 Summed absolute pressure difference according to filling levels.

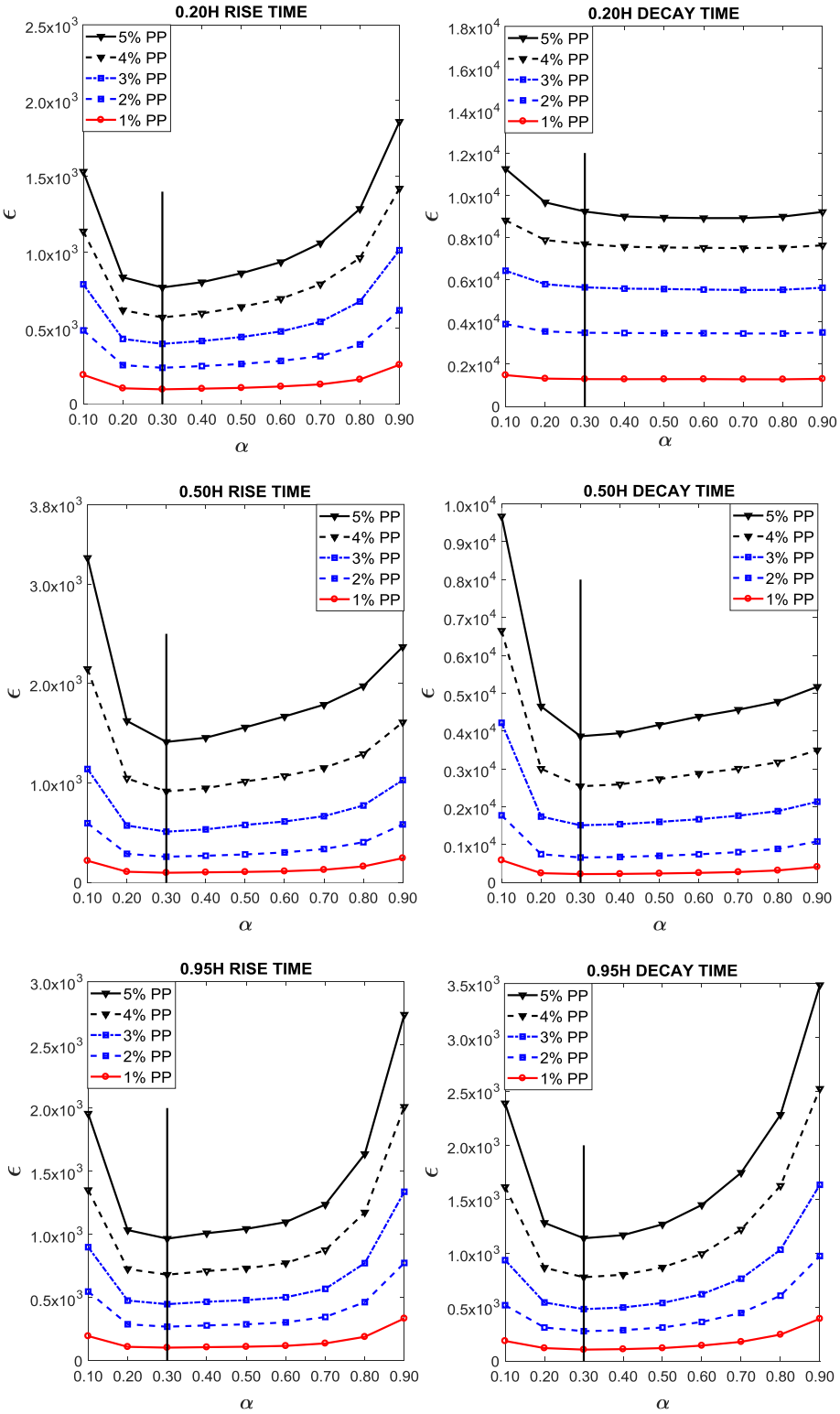

Fig. 4.17 Summed absolute pressure difference in highest peak pressures in each filling level.

5. Conclusion

In this thesis, statistical analysis of sloshing impact pressures and analysis on triangular modelling of impact pressure signals are carried out. Weibull, generalized Pareto, generalized extreme value and log-logistic distributions fitted by different parameter estimation methods are evaluated for short term and long term prediction. In the next part, a comparison of pressure ratios is carried out for an accurate triangular modelling of peak pressure signals.

Choice of statistical model is an important subject in the design load selection of LNG tanks. For short term distribution, different statistical models may return relatively closer estimates of maximum pressure, however, for long term prediction the estimates vary significantly. Through this research, it was seen that, not only the choice of statistical distribution but also choice of distribution fitting method makes a great difference in terms of estimated maximum pressure. It can be considered as a parameter that affects the shape of the distribution. Therefore, the choice of statistical distribution should be considered in this larger frame. In this research, maximum-likelihood estimation is concluded to be a weak method to be used with three-parameter distributions.

In distribution fitting, various goodness-of-fit tests are applied in previous studies to evaluate how well the fit follows the data. However, in case of sloshing impact pressures, it is more important to evaluate how well the fit follows a more converged data. A good fit to the data does not mean it will return closer estimates of maximum pressure in longer return periods. Therefore, testing goodness-of-fit according to the data used for fitting can be misleading in case of sloshing peak pressures.

Taking 100hrs test data as a reference and considering 5hrs test data estimated pressures, in 20% filling level, log-logistic distribution fitted by method-of-moments and l-moments method; in 50% filling level, log-logistic distribution fitted by method-of-moments and l-moments method, and generalized extreme value distribution fitted by l-moments method; and in 95% filling level, log-logistic distribution fitted by method-of-moments and l-moments method, provide the closest pressure estimates according to applied squared error approach. Beyond this numerical evaluation, long term plotting presents how each fit behaves compared to long duration test data. From these observations, it was understood that, generalized Pareto follows the tail of the data so well that, in most cases, it is impossible for it to return consistent and close estimates. The reason is simply because it is affected by the tail data significantly. Weibull distribution also follows the whole data smoothly and the estimations heavily depend on the data set used in each case. Therefore, the deviation of estimated maximum pressure is large from one case to another. On the other hand, generalized extreme value fitted by l-moments method and log-logistic distributions tend to preserve their shapes, showing small tendencies of indifference to the data sets, which leads to consistent estimates. Therefore, the observations from long term plotting are in agreement with the results of squared error approach. Among these 3 fits that return consistent estimates, log-logistic distribution fitted by method-of-moments is seen to return closest estimates if overall results are considered. A further discussion can be made about the behavior of log-logistic distribution in much longer return periods.

In triangular modelling of peak pressure signals, results show that in 20% filling level rise time and 50% and 95% filling levels rise and decay times, pressure ratio of 0.30 is the nearest idealization to the actual signal. In 20% filling level decay time, there is no obvious pattern of pressure ratio for triangular modelling. Actually, 50% and 90% filling levels decay times

having an obvious is an unexpected result. If pressure signals are observed, it can be seen that rising pressure signals have small irregularities and mostly have a clean rise until peak value. Decaying pressure signals, on the other hand, usually contain local peaks, are very irregular and difficult to classify. Therefore, 50% and 95% decay times having an obvious pattern is an unexpected result given these irregularities.

Considering both choice of statistical distribution and peak signal modelling, the results are hardly in accordance with the current procedure of classification societies. Hopefully, contents of this research raise attention on these important matters regarding sloshing impact pressures.

Bibliography

[1] American Bureau of Shipping, 2006, *Guidance Notes On Strength Assessment of Membrane-Type LNG Carrier*, Guidance Note (updated in 2014), Houston, USA.

[2] Bureau Veritas, 2011, *Design Sloshing Loads for LNG Membrane Tanks*, Guidance Note, Neuilly sur Seine Cedex, France.

[3] Cousineau, D., 2009, 'Nearly Unbiased Estimators for the Three Parameter Weibull Distribution with Greater Efficiency than the Iterative Likelihood Method', British Journal of Mathematical and Statistical Psychology, 62, 167-191.

[4] Cunnane, C., 1978, 'Unbiased Plotting Positions – A Review', Journal of Hydrology, Vol. 37(3/4), 205-222.

[5] Det Norske Veritas, 2014, *Sloshing Analysis of LNG Membrane Tanks*, Classification Notes, Oslo, Norway.

[6] Filliben, J.J., 1975, 'The Probability Plot Correlation Coefficient Test For Normality', Technometrics, 17(1), 111-117.

[7] Fillon, B., Diebold, L., Henry, J., Derbanne, Q., Baudin, E., Parmentier, G., 2011, 'Statistical Post-Processing of Long-Duration Sloshing Test', Proc 21th Int Offshore and Polar Eng Conf, ISOPE, Maui, Hawaii, 46-53.

[8] Grazcyk, M., Moan, T. and Rognebakke, O., 2006, 'Probabilistic Analysis of Characteristic Pressure for LNG Tanks', Journal of Offshore Mechanics and Arctic Engineering, 128, 133-134.

[9] Grazcyk, M. and Moan, T., 2008, 'A Probabilistic Assessment of Design Sloshing Pressure Time Histories in LNG Tanks', Ocean Engineering, 35, 834-855.

[10] Gran, S., 1981, ‘Statistical Distributions of Local Impact Pressures’, Norwegian Maritime Research, 8(2), 2-13.

[11] Heo, J-H, Kho, YW, Shin, H, Kim, S., 2008, ‘Regression Equations of Probability Plot Coefficient Test Statistics from Several Probability Distributions’, Journal of Hydrology, 355, 1-15.

[12] Hosking, J.R.M., 1990, ‘L-Moments: Analysis and Estimation of Distributions Using Linear Combinations of Order Statistics’, Journal of Royal Statistical Society Series (B) Method, 52(1), 105-124.

[13] Hosking, J.R.M, Wallis, J.R. and Wood, E.F., 1985, ‘Estimation of the Generalized Extreme Value Distribution by the Method of Probability-Weighted Moments’, Technometrics, Vol. 27.

[14] Kim, S.Y., Kim, Y., Kim, K.H., 2014, ‘Statistical Analysis of Sloshing-Induced Random Impact Pressures’, Proc Inst Mech Eng, Part M: Journal of Engineering for the Maritime Environment, 228(3), 235-248.

[15] Kim, S.Y., 2017, ‘Development of Long-term Prediction Procedure and Outlier Analysis for Sloshing Impact Loads on LNG Cargo Tank’, PhD Thesis, Seoul National University, Seoul, South Korea.

[16] Kuo, J.F., Campbell, R.B., Ding, Z., Hoie S.M., Rinehart, A.J., Sandstrom, R.E. and Yung, T.W., 2009, ‘LNG Tank Sloshing Assessment Methodology – The New Generation’, Int Journal of Offshore and Polar Eng, ISOPE, 19(4), 241-253.

[16] Lloyd’s Register, 2009, Sloshing Assessment Guidance Document for Membrane Tank LNG Operations, London, UK.

[18] Mathiesen, J., 1976, ‘Sloshing Loads Due to Random Pitching, ‘Norwegian Maritime Research, 3(2), 2-13.

[19] Myung, I.J., 2003, ‘Tutorial on Maximum Likelihood Estimation’, Journal of Mathematical Psychology, 47, 90-100.

[20] Pickands, J. III., 1975, ‘Statistical Inference Using Extreme Order Statistics’, Ann Stat, 3(1), 119-131.

[21] Rognebakke, O.F., Hoff, J.R., Allers, J.M., Berget, K., Berge, B.O., Zhao, R., 2005, ‘Experimental Approaches For Determining Sloshing Loads In LNG Tanks’ Proc of SNAME Annual Meeting, Houston, Texas, USA.

[22] Smith, R.L., 1985, ‘Maximum Likelihood Estimation in A Class Of Nonregular Cases’, Biometrika, 72, 67-90.

[23] Vogel, R.M., 1986, ‘The Probability Plot Correlation Coefficient Test for Normal, Lognormal, and Gumbel Distributional Hypotheses’, Water Resources Research, 22(4), 587-590.

초록

본 논문은 슬로싱 실험을 통하여 계측된 슬로싱 충격압력 통계해석과 충격압력 신호 모델링 해석을 다루고 있다. 90년대 후반부터 LNG 시장의 변화로 인해 LNG선이 점차 대형화되었고, LNG 저장 탱크의 개수는 동일하기 때문에 탱크의 크기가 점차 커지게 되었다. 또한, 전 세계에 FPSO 사용이 증가함에 따라 on-off-loading 중에 LNG선이 겪는 기상조건이 심해지게 되었고, 이로 인해 LNG선에서의 슬로싱 문제가 대두되었다.

슬로싱 문제의 해석으로는 실험적 접근법과 수치적 접근법으로 나뉠 수 있다. 슬로싱은 불규칙적이고 복잡한 운동이기 때문에 수치적 계산하기 위해서는 많은 시간과 노력이 필요하다. 그러므로 슬로싱 실험이 슬로싱 충격압력 해석과 수치적 계산의 기준으로 널리 사용되고 있다.

LNG 탱크의 설계 단계에서 사용되는 최대압력값 예측을 위해서는 슬로싱 실험의 충격압력 신호에서 얻어진 추출시간간격과 임계 압력값으로 계측된 압력값들의 통계해석이 필요하다. 이때 압력값을 어떤 분포함수로 표현하는지가 매우 중요한 과정이라고 할 수 있다. 현재 선급 규칙과 연구 기관들에서는 주로 Weibull 분포함수와 generalized Pareto 분포함수가 사용된다. 하지만, long term prediction을 고려하기 위해서 이 외의 다른 분포함수에 대한 연구가 필요하다.

슬로싱 문제에서 또 다른 중요한 문제는 충격압력 신호를 모델링하는 방법이다. LNG 탱크의 내부요동 공진주기와 선박의

공진주기가 가까울수록 공진의 가능성이 커진다. 또한, 신호의 상승과 하강시간이 구조적 응답에 영향을 주기 때문에 충격압력 신호의 모델링은 탱크의 설계에 있어 매우 중요한 과정이라고 할 수 있다. 현재 선급 규칙과 연구 기관들에서는 주로 압력값의 2분의 1 값을 지나가는 삼각형 모델링이 사용되고, 따라서 이 부분에서도 더욱 자세한 연구가 필요하다.

본 논문에서 첫 번째 내용으로는 3차원 실선 모델에 대한 슬로싱 모형실험을 통해 얻은 충격압력 값들의 통계해석을 수행하였다. 슬로싱 모형실험의 데이터로는 20%, 50%와 95% 적재수심에서 동일조건의 실선기준 5시간 실험을 20회 반복한 데이터를 사용하였다. 이러한 충격압력 값을 이용하여 다양한 분포함수로 distribution fitting을 수행하였고, 이에 따른 결과로부터 가장 잘 맞는 4개의 분포함수를 선정하였다. 선정된 분포함수들은 Weibull, generalized Pareto, generalized extreme value와 log-logistic 분포함수다. 이 4개의 분포함수에 대하여 최대 3가지 각기 다른 방법으로 distribution fitting을 수행하였다. 얻은 fit에 대해서 초과확률 커브와 goodness-of-fit 테스트 (PPCC 테스트)를 통해 비교하였다. 또한, 100시간 실험 데이터를 기준으로 5시간 실험 데이터 fitting의 squared error 값을 비교하였다. 또한, 100시간 실험 데이터를 기준으로 현재 선급 규칙에 따라 추정되는 압력 값과의 차이를 비교하였다. 100시간 실험 데이터는 동일조건에서 실선기준 5시간 실험을 20회 반복을 한 데이터를 취합하였다.

본 논문에서 두 번째 내용으로는 충격압력 신호 모델링에 대한 해석을 수행하였다. 이를 위해 실제 신호에서 9개의 압력값

비율에 대해 상승시간과 하강시간을 계산한 후 각 압력값 비율에서의 삼각형 모델링을 통해 얻은 상승시간과 하강시간과의 차이의 절댓값을 더해서 비교하였다. 또한, 각 적재수심과 각 적재수심에서 중요한 패널에 대해 20회 반복 수행한 실험 결과와 모든 충격압력 신호에 대해 압력값 개수를 기준으로 10%씩 나눠서 결과를 비교해 보았다. 이러한 결과를 통해 충격압력 신호 삼각형 모델링에서 사용된 압력값 비율을 제안하였다.

주요어: 슬로싱, 충격압력, 통계해석, 모형실험, 신호 모델링.

학번: 2015-23297